

Interface Properties of Geogrid and Fly Ash/Fly Ash-Tire Chip Mixtures

K P Bhargav Kumar

A Dissertation Submitted to
Indian Institute of Technology Hyderabad
In Partial Fulfillment of the Requirements for
The Degree of Master of Technology



भारतीय प्रौद्योगिकी संस्थान हैदराबाद
Indian Institute of Technology Hyderabad

Department of Civil Engineering

July, 2014

Declaration

I declare that this written submission represents my ideas in my own words, and where others' ideas or words have been included, I have adequately cited and referenced the original sources. I also declare that I have adhered to all principles of academic honesty and integrity and have not misrepresented or fabricated or falsified any idea/data/fact/source in my submission. I understand that any violation of the above will be a cause for disciplinary action by the Institute and can also evoke penal action from the sources that have thus not been properly cited, or from whom proper permission has not been taken when needed.



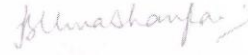
(Signature)

K P Bhargav Kumar

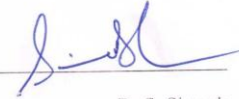
CE12M1006

Approval Sheet

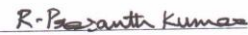
This thesis entitled '*Interface Properties of Geogrid and Fly Ash/Fly Ash-Tire Chip Mixtures*' by K P Bhargav Kumar is approved for the degree of Master of Technology/ Doctor of Philosophy from IIT Hyderabad.



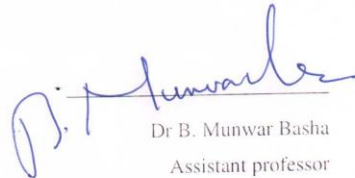
Dr B. Umashankar
Assistant professor
Department of Civil Engineering
Indian Institute of Technology Hyderabad



Dr S. Sireesh
Associate professor
Department of Civil Engineering
Indian Institute of Technology Hyderabad



Dr R. Prashanth Kumar
Assistant professor
Department of Mechanical & Aerospace Engineering
Indian Institute of Technology Hyderabad



Dr B. Munwar Basha
Assistant professor
Department of Civil Engineering
Indian Institute of Technology Hyderabad

Acknowledgements

The research samples are collected from Neyveli thermal power plant and Ramagundam thermal power plant. I would like to thank the officials at the two power plants for their cooperation in collecting the samples. I would like to thank my advisor Dr.B.Umashankar for his candid and unbiased support throughout my research.

I would like to extend my gratitude to my brother Mr. K P Kishore Kumar and my parents for their invaluable support in completing my Master's degree.

I would like to extend my special thanks to Hari Prasad and my classmates Prashant, Sarath and Akhila.

I would also like to thank my friends Sasanka Mouli, Saranya, Vinay, Bhagath, Vijay Kumar, Thejesh, Ugesh, Durga Prasad, Chandra Sekhar, Chiranjeevi, Harish, V Santhosh, Dan, Damodhar, Karthik, Thulasi Ram, Sandeep, Rukmini for their helping hands in completing the project.

I would like to thank Vijay for helping out in doing the lab experiments.

Dedicated to

My Brother & Parents

Abstract

Disposal of waste materials like fly ash and tire chips is a major environmental concern. One of the possible applications of these waste materials is to utilize them as backfill materials in Mechanically Stabilized Earth (MSE) walls. The common modes of failure in MSE walls are (a) pull out mode of failure, and (b) sliding mode of failure. The sliding mode of failure can be studied by performing interface tests in the direct shear box to know the interface or sliding shear resistance offered by the reinforcement with respect to the soil under a given surcharge loading. In this study, it is proposed to use fly ash, and mixtures of fly ash and shredded tires as a backfill material. Hence, this study is carried out to quantify the interface shear resistance between the geogrid reinforcement and fly ash-tire chips mixtures. Ash from two different sources, Neyveli Thermal Power Plant and Ramagundam Thermal Power Plant, are used to study the interfacial shear strengths. The interface properties are also compared with the conventional fill material (like sand) and are found to be comparable. Four different percentages by weight of tire chips are mixed with fly ash (0%, 10%, 30% and 60%, by weight of dry fly ash) to prepare the mixtures. 30% and 60% mixes showed higher shear strength in the case of both the ashes. 30% mixtures are found to give higher interfacial shear strength in the case of Neyveli Coarse fly ash, and almost equal strengths for 30% and 60% additions in the case of Ramagundam Pond ash. The interaction efficiency of geogrid and both the ashes are calculated and is found to be in the range of 80-130% (with respect to cohesion and friction angles), and for the tire chips mixed ashes it is found to be in the range of 40-150% (with respect to cohesion and friction angles). The interaction coefficients between geogrid and fly ash is found to be in the range from 0.85-0.95, and for geogrid and fly ash-tire chips mixtures is found to be in the range of 0.75-0.98. This study suggests that the sliding resistance of geogrid reinforced ash is comparable with that of conventional fill material, and hence can be a competent material for backfill applications.

Nomenclature

NFA – Neyveli Coarse fly ash

RPA – Ramagundam Pond Ash

SP – Poorly-graded sand

SP-SM – Poorly-graded sand with silty sand

XRF – X-ray fluorescence

SEM – Scanning electron microscope

C_u – Coefficient of uniformity

C_c – Coefficient of curvature

TC – Tire chips

FESM – Field Emission Scanning Electron Microscope

D_{10} – Effective particle size

D_{30} – Particle size corresponding to 30% finer

D_{60} – Particle size corresponding to 60% finer

D_{50} – Average particle size

C – Apparent cohesion between the soil to soil particles

Φ – Friction angle

C_a – Adhesion between the geogrid and soil particles

δ – Interface friction angle

R_i – Interface interaction coefficient

E_c – Efficiency of geogrid with respect to cohesion

E_ϕ – Efficiency of geogrid with respect to friction

Contents

Declaration.....	ii
Approval Sheet	iii
Acknowledgements.....	iv
Abstract.....	vi
Nomenclature	vii
1 Introduction.....	1
1.1 Problem statement.....	1
1.2 Research Motivation, Objectives and Scope.....	2
1.3 Research Approach.....	4
1.4 Report Outline.....	4
2 Literature Review	5
2.1 Overview.....	5
2.2 Handling and disposal of coal ashes	6
2.3 Fly ash utilization.....	7
2.4 Physical properties	8
2.4.1 Specific gravity.....	8
2.4.2 Gradation	8
2.5 Chemical properties	8
2.5.1 Chemical composition.....	8
2.5.2 X-ray diffraction and morphology.....	9
2.5.3 pH.....	9
2.5.4 Lime reactivity	9
2.6 Engineering properties.....	10
2.6.1 Shear strength of coal ashes	10
2.6.2 Compressibility	11
2.6.3 Permeability.....	11
2.7 Review on interfacial shear tests and direct shear tests	11
2.8 Studies on fly ash and bottom ashes	14
3 Experimental work	15
3.1 Raw materials used	15
3.1.1 Neyveli fly ash.....	15

3.1.2	Ramagundam pond ash.....	16
3.1.3	Sand.....	17
3.1.4	Geogrid.....	17
3.1.5	Tire chips.....	18
3.2	Experimental setup.....	19
3.3	Tests conducted.....	21
3.3.1	Grain size analysis.....	21
3.3.2	Specific gravity.....	22
3.3.3	Standard Proctor compaction test.....	23
3.3.4	SEM analysis.....	23
3.3.5	Chemical composition.....	23
3.3.6	Direct shear and interfacial shear tests.....	24
3.4	Fly ash-tire chips mixture.....	26
4	Results and Discussions.....	28
4.1	Test results on sand.....	28
4.1.1	Grain size distribution.....	28
4.1.2	Specific gravity.....	29
4.1.3	Standard Proctor compaction test.....	29
4.1.4	Morphology.....	30
4.1.5	Results of direct shear and interfacial tests.....	30
4.2	Test results on Neyveli fly ash.....	33
4.2.1	Grain size distribution.....	33
4.2.2	Specific gravity.....	34
4.2.3	Standard Proctor compaction test.....	34
4.2.4	Morphology.....	35
4.2.5	Chemical composition.....	35
4.2.6	Direct shear and interfacial tests.....	35
4.3	Test results on Ramagundam pond ash.....	37
4.2.1	Grain size distribution.....	37
4.2.2	Specific gravity.....	38
4.2.3	Standard Proctor compaction test.....	38
4.2.4	Morphology.....	39
4.2.5	Chemical composition.....	39
4.2.6	Direct shear and interfacial tests.....	39
4.4	Comparisons of shear strengths of sand, NFA and RPA.....	41

4.5 Tire chips	43
4.6 Tire chips and NFA, RPA mixtures.....	44
5 Conclusions.....	56
References.....	58

Chapter 1

Introduction

1.1 Problem statement

Fly ash is one of the most useful waste materials. According to the census conducted by Central Electricity Authority, New Delhi, nearly 163 million tons of fly ash is being produced annually across India (Central Electricity Authority 2014). This amounts to nearly 30 percent of fly ash that is produced across the world. Large quantity of ash is produced in India because of the type of the coal that is used. Indian coal is categorized as low-grade coal with high ash content of nearly 40% in comparison to that of imported coal that contains ash content of only 10-15%. Fly ash has many applications in civil engineering, for example, fly ash is used in the preparation of cement and bricks, as a fill material for roads and embankment constructions, as fill material for reclamation and mine filling, as fertilizer in agricultural fields, etc.

According to the report published by the Central Electricity Authority, New Delhi, India, on fly ash generation at coal-fired thermal power stations, the utilization of fly ash was 100 million tonne over the production of 163 million tonne leading to its utilization of about 56% in the year 2012-13. Utilization of fly ash is 41.1% in cement sector, 11.7% in reclamation of low lying area, 6% in roads and embankments, 10.3% in mine filling, and 9.94% in building materials like bricks, tiles etc. (Central Electricity Authority 2014). As per the report, the utilization of fly ash in cement sector has increased from 2.4 million tonne in 1998-99 to 41.3 million tonne in 2012-13. Similarly, utilization of fly ash used in reclamation of low lying areas has increased from 4.1 million tonne in 1998-99 to 11.8 million tonne in 2012-13, and its utilization increased from 1.1 million tonne of fly ash in 1998-99 to 6.0 million tonne in 2012-13 in the construction of roads and embankments. Overall, the fly ash utilization has increased from 9.6% during 1996-97 to 61.3% during 2012-13(Central Electricity Authority 2014). However, it is essential to find applications

that can result in large-volume consumption of fly ash. One such application is use of fly ash as a fill material in embankment construction.

Tire chips are one other waste material that possesses favorable properties required of a fill material. There is steady increase in the production of scrap tires across the world. Nearly 300 million scrap tires per year were produced in the USA in the year 2012-2013 (Rubber Manufacturers Association 2013, and American Recycler News Inc. 2013), 260 million passenger car tires in the European Union in the year 2003 (Shulman 2004), 106 million tires in Japan in 2006 (Japan Automobile Tire Manufacturers Association 2007) and 112 million scrap tires per year in India (Rao and Dutta 2006). Tire chips are light weight, thermally resistive and free draining which are favorable properties for their usage in civil engineering applications. Typically, whole scrap tires are shredded to smaller size tire shreds (with sizes ranging from 10 to 300mm) and mixed with sand to improve the properties of the composite material. Tire chips/shreds are non-biodegradable and can be utilized in many geotechnical engineering applications.

This study involves the use of fly ash, and composite material of fly ash and shredded tires as a backfill material in reinforced earth structures. The common modes of failure in mechanically stabilized earth walls (MSE) walls are (a) pull out mode of failure, and (b) sliding mode of failure (Tuna and Altun 2012). The sliding mode of failure can be studied by performing interface tests in the direct shear box to know the interface or sliding shear resistance offered by the reinforcement with respect to the soil under a given surcharge loading.

This study involves investigation on the interface shear strength of the geogrid and fly ash, and geogrid and shredded tires-fly ash mixtures. Fly ash is obtained from two sources- Neyveli Thermal Power Plant, and Ramagundam Thermal Power Plant. Neyveli Thermal Power Plant produces two gradations of fly ash- coarse and fine. In this study, coarse fly ash is used. Fly ash that is collected from Ramagundam Thermal Power Plant is pond ash.

1.2 Research Motivation, Objectives and Scope

Fig.1.1 shows the reinforced backfill along the kinematics of sliding failure of reinforcement against the backfill material (in enlarged view). Tire chips provide higher shear strength when mixed with the soil and offers good drainage properties (Attom 2005). This study focuses mainly on the fly ash and geogrid interaction at the interface and the failure associated with sliding mode. Experimental study is carried out to obtain the interface shear strength of geogrid and fly ash, and geogrid and fly ash-tire shred mixtures.

A comparison is also made with the interface shear strength of geogrid and sand. The interfacial shear resistance is mainly offered by the interaction of soil and surface of geogrid ribs, interaction of soil particles in the openings of geogrid, and the passive resistance against the transverse ribs.

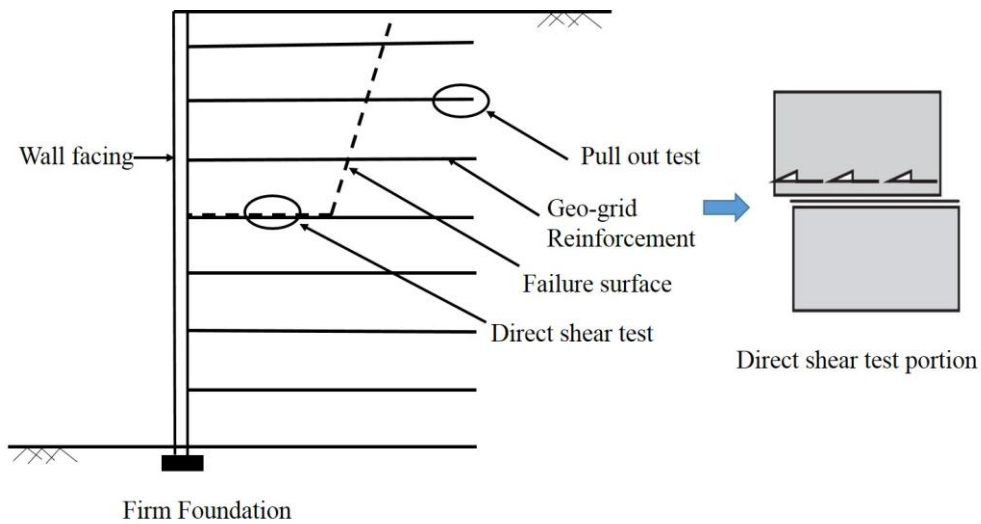


Fig 1.1 Schematic showing pull out and sliding failure modes (Palmeria 2009)

Fig.1.2 shows a schematic of interface test between reinforcement and soil under an applied normal load using a direct shear apparatus.

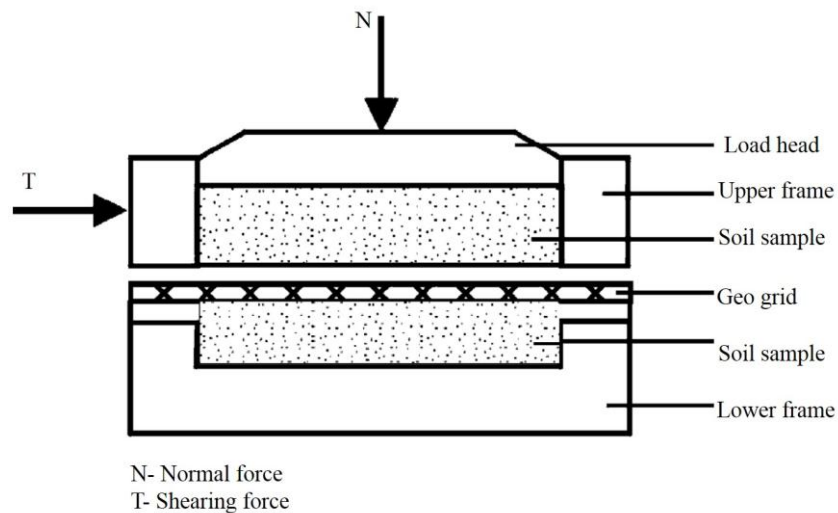


Fig 1.2 Schematic of interface test (Adamska 2006)

For interface testing on geogrid and the mixtures, the mix proportions included tire chip contents equal to 10%, 30%, 60% (by weight of fly ash). The results are presented in the form of interface shear strength envelopes that can be useful in the design of MSE walls with fly ash or composite material of fly ash and tire chips as backfill material.

1.3 Research Approach

An experimental test program was undertaken to conduct characterization tests (gradation, specific gravity, compaction characteristics, chemical composition, morphology, etc.), and interface shear strength testing. These tests were done on fly ash obtained from two sources and locally available sand. Testing was then extended to mixtures of tire chips and fly ash.

1.4 Report Outline

Chapter 2 reviews the literature available on characteristics of fly ash and shredded tires, and studies on pullout or interface testing of geosynthetic and fills.

Chapter 3 gives a brief introduction on the raw materials used in the study, and the experimental procedures adopted to perform characterization tests on raw materials and direct shear testing procedures.

Chapter 4 covers the results and discussions from characterization studies, direct shear and interfacial testing.

Chapter 5 outlines the conclusions drawn from the study.

Chapter 2

Literature Review

2.1 Overview

Fly ash is one of the residues generated in the process of combustion of coal in thermal power plants. It comprises of fine particles that rise with flue gases, hence it is also called as flue ash. Fly ash is generally collected in electro static precipitators or other particle filtration equipment before the flue gases reach the chimneys of coal-fired power plants. The ash that cannot fly will be collected from the bottom of the furnace, and is termed as bottom ash. Fly ash together with Bottom ash is known as pond ash (Kim et al. 2005).

Coal ash is primarily composed of silica (SiO_2), ferric oxide (Fe_2O_3) and alumina (Al_2O_3), and smaller quantities of calcium oxide (CaO), potassium oxide (K_2O), sodium oxide (Na_2O), magnesium oxide (MgO), titanium oxide (TiO_2), phosphorous pentoxide (P_2O_5), and sulphur trioxide (SO_3) (Kim et al. 2005).

In general coals can be classified into four groups, viz., anthracite coal, Bituminous coal, sub-bituminous coal, and lignite coal.

Anthracite coal is the superior grade of coal. Anthracites are clean, dense, and hard. Hence, these are also called as hard coals. They have high percentage of carbon (about 90%) and low percentage of volatile matter. They are difficult to ignite. However, once ignited they burn for long time with clean flame with almost smokeless. They can produce very high temperature. Bituminous coal is usually black to dark brown in color. They have 75% - 90% carbon and less than 20% of moisture content. These coals ignite relatively easily, and burn with a long flame. Sub-bituminous coal is moist when they are fresh. They break easily once

they get exposed to atmosphere. They contain about 60%-80% carbon. Sub-bituminous coals ignite easily, and once ignited they burn with a medium flame with little smoke or soot. Lignite coal, also known as brown coal, is the lowest grade coal. It is brownish in color, and wood like in structure. It contains high moisture content about 30%-75%, and breaks up easily upon drying like sub-bituminous coal. The carbon content varies in the range of 55% - 73%. They have a high ash content of about 45%. Lignite coals ignite easily, and burns with little smoke.

2.2 Handling and disposal of coal ashes

Fly ash that is produced in thermal power plants can be handled in three ways

1. Mechanical handling: In this system, ash is collected at the bottom of mechanical dust collector or electrostatic precipitator (ESP), and taken to closed wagons or bags through tourniquets or rotary valves. This method is used where the quantity of fly ash to be handled is small.
2. Pneumatic handling: In this method, the fly ash is transferred to a central storage silo with the help of air currents.
3. Hydraulic handling: In this system, the fly ash from the hoppers of the mechanical dust collector or ESP is made to enter a flush apparatus, which discharges it in the slurry form to a sump from where it is conveyed to the disposal area with the help of pumps, or the slurry collected at the sump is lifted and transported to a de-watering concrete storage bin with the help of pump where the separation of ash and water takes place.

When pulverized coal is burnt, about 80% of the unburned material is entrained in the flue gases, and is collected as fly ash. The remaining 20% which is coarser in size is collected from the bottom of the furnace, known as bottom ash.

The fly ash that is collected in the dust collectors or ESP's or from silos is collected in dry or moist form based on the quality. If the quality of fly ash is good, it is collected in dry form in closed wagons or in moisture proof bags and transported to the areas of utilization of fly ash. If the quality of the fly ash is not good, it is conditioned with requisite amount of moisture to control the dust in order to reduce environmental pollution. This fly ash is called as conditioned fly ash.

Dry disposal of fly ashes has many disadvantages like

- Pollutes the atmosphere as it gets air borne due to its lightweight.
- Causes diseases like silicosis, allergic bronchitis and fibrosis of lungs on long breathing of fly ash
- Spoils the characteristics of top soil when it is deposited over an area.

- Corrodes the structural surfaces, and contaminates the surface water as well as ground water which may affect the aquatic life.

Even the wet disposal that is practiced over the world has the following disadvantages like

- Affects the pozzolanic behavior.
- Affects the surface water and aquatic life.
- Causes harm to plants due to usage of water from ash ponds.
- Consumes more area of land needed for disposal.

Proper care during planning, designing, construction and maintenance of ash disposal systems reduces the effects of fly ash. Some of the measures are

- Locating the ash disposal as far as possible away from the habitats.
- Ensuring the wind blows in the direction towards the disposal area and not towards the habitats.
- Providing the vegetation as a cover over the ash mound.
- Sprinkling of water at a controlled rate during the construction of mound.
- Locating the ash mounds over soil deposit with low permeability.

2.3 Fly ash utilization

Based on the utilization of fly ash, it can be categorized as three groups like low value utilization, medium value utilization, and high value utilization.

Usage of fly ash in embankment construction, dams, mine fillings, back filling, structural filling, road construction, soil stabilization, mass concreting, ash dykes comes under the low value utilizations.

Usage in manufacturing of pozzolanic cement, fly ash concrete, cellular cement, bricks, light weight aggregate, grouting, and soil fertilizers comes under the medium value utilizations.

High value utilization covers the usage of fly ash in metal recovery, in ceramic industry, floor and wall tiles, fly ash distempers and paints.

Almost 60% of fly ash can be disposed effectively if planned and executed for low value utilizations. For this, the understanding of various properties like physical, chemical and engineering properties are important.

To deal with the advantages and disadvantages of fly ash, the various properties like chemical, physical and engineering properties should be studied.

2.4 Physical properties

The various applications of fly ash in various fields like in embankment construction, and as a backfill material is possible only with the proper knowledge of physical properties like size, structure, gradation, specific gravity etc.

2.4.1 Specific gravity

Specific gravity is one of the important properties required in efficiently planning the fly ash utilization in bulk quantities. The specific gravity of fly ashes in India widely varies between 1.66 and 2.55 (Sridharan et al. 2001a). The specific gravity increases with the content of iron oxide. With the fineness of fly ash, the specific gravity increases (Trivedi and Sud 2004). The other factor which affects the specific gravity is the presence of cenospheres. Cenospheres are light weight, inert, hollow spherical particles made of silica and alumina and filled with air or inert gas. The specific gravity of fly ashes are comparatively low when compared to that of soils that lie in a narrow range of 2.6-2.8. The specific gravity of fly ash is determined using ASTM D854 (2000) (Method A) or IS: 2720-Part 3/Sec 1 (1980).

2.4.2. Gradation

Size is another important aspect to know about fly ash while planning and executing the geotechnical projects. Grain-size distribution provides information whether the fly ash is coarse grained or fine grained, and also whether they are well graded or poorly graded. The grain size analysis can be done according to IS: 2720-part 4 (1985). The size of the Indian fly ash particles generally varies between $0.5\mu\text{m}$ – $300\mu\text{m}$. This is in the range of silt and fine sand. The gradation of the particles is decided based on the values of coefficient of curvature C_c , and coefficient of uniformity C_u . For C_u value greater than 6 and C_c between 1 and 3, the ash is considered as well graded, otherwise as poorly graded. As the ash becomes finer, the C_u value decreases. Most of the Indian fly ashes are poorly graded (Sridharan et al. 2001a).

2.5 Chemical properties

Like the physical properties, the chemical properties also play a crucial role in influencing the behavior of fly ashes. The basic composition of ash, pH, morphology, and lime reactivity are some of the chemical properties which affect the strength and behavior of fly ash. The following sections explain each of these properties in brief.

2.5.1 Chemical composition

As mentioned in the previous section, ashes are produced from coal, and hence the chemical composition of the ash mainly depends on the quality, chemical composition of the parent

coal, method of burning and combustion processes, the additives used for flame stabilization, corrosion control additives used, hopper position, flow dynamics of the precipitators and the removal capacity of pollution control devices (Sridharan & Prakash, 2007, p.10). The principal constituents of coal ash are silica (SiO_2), alumina (Al_2O_3) and ferric oxide (Fe_2O_3). Oxides of calcium, magnesium, sulphur, titanium and sodium are also present in small amounts. Indian fly ashes contain about 38-65% silica, 16-44% alumina and 3-20% ferric oxide (Sridharan et al. 2001b). Indian bottom ashes contain about 23-73% silica, 13-27% alumina and 3-11% ferric oxide (Sridharan et al. 2001b). Indian pond ashes contain about 37-75% silica, 11-54% alumina and 3-35% ferric oxide (Sridharan et al. 2001b). In general, fly ashes contain higher silica than alumina. However, class-C fly ash differs from this trend because of its pozzolanic and self-cementing properties.

2.5.2 X-ray diffraction and morphology

This study indicates that the coal ashes predominantly contain quartz and feldspar minerals, the carbonates and chlorites to a lesser extent. The x-ray diffraction spectra indicate that the fly ashes contain both amorphous and crystalline phases of materials, having amorphous phase around 90% or even more. The morphological studies for coal ashes when done through a Scanning Electron Microscope (SEM) suggests that they are solid spheres, hollow spheres, sub-rounded porous grains, irregular agglomerates, and irregular porous grains of unburned carbon. If iron compounds are present, they can be spotted as angular or opaque spheres. Cenospheres constitute a good proportion of coal ash (about 5-10% by volume). Bottom ashes are generally angular as they are coarser in texture. Pond ashes have both spherical and angular particles (Sridharan et al. 2001b).

2.5.3 pH

In general, about 95% of the fly ash comprises of non-toxic compounds of silicon, aluminum, iron and calcium in addition to small quantities of oxides of magnesium, sodium and potassium. Hence, most of the fly ashes are alkaline in nature. pH of coal ashes varies in the range of 3 to 12, depending on the alkaline content and free lime content. Higher the lime content, higher is the pH.

2.5.4 Lime reactivity

Lime reactivity is the property in which metastable silicates are present in all the fly ashes, even those which possess little or no cementing value, react with the calcium ions in the presence of moisture to form water insoluble calcium silicates and aluminum silicates. It depends on the quantity of reactive silica that is in amorphous form, free lime, iron and unburned carbon contents and their specific surface area. Silica which is soluble in 3N

Hydrochloric acid is taken as reactive silica. The lime reactivity is generally assessed by performing compressive strength of standard mortar cubes in accordance with IS: 1727, 1967. This strength is determined for both the fresh samples and aged samples. Most of the aged samples show the maximum lime reactivity. In general, fly ashes will have higher reactivity compared to bottom ashes or pond ashes.

2.6 Engineering properties

Engineering properties mainly include the shear strength, compressibility and permeability. They play an important role in selection of fly ash for applications in geotechnical engineering. In order to study the engineering properties, it is important to know the effect of compaction on the sample which controls the engineering properties. The compaction characteristics of the fly ash are important to study its applications in geotechnical field. The dry density of the sample is a measure of degree of compaction.

The study of compaction curves of coal ashes indicates the following:

1. Trend is similar to that of soils. It exhibits a dumb-bell shaped compaction curve identical to granular soils, i.e., like sand. While for finer fly ashes, the density variation with water content is similar to that of silty clays (Sridharan et al. 2001c).
2. Compaction curves are relatively flatter showing that all the coal ashes are water insensitive.
3. The dry unit weight at air dried state is generally higher than the maximum dry unit weight at optimum moisture content.
4. The compaction curve of class-C fly ash occupies lowest position in comparison with other curves -attributing to the increased resistance offered by the pozzolanic reaction compounds that are formed at the mixing stage itself (Sridharan et al. 2001c).
5. Coarser coal ash has higher OMC and lower dry density, while finer coal ash exhibits a lower OMC and higher dry density (McLaren and DiGioia 1987). This is where the coal ashes differ from the normal soils. This is peculiar behavior with the coal ashes. This may be explained considering the gradation, chemical composition and physico-chemical nature of soils and coal ashes.

2.6.1 Shear strength of coal ashes

Shear strength plays a crucial role in understanding the problems regarding bearing capacity, slope stability of embankments, design of pavements and retaining structures. Shear strength tests for coal ashes are done similar to that of soils in both drained and undrained conditions. Conventional shear tests can be done on coal ashes. In spite of low

densities, coal ashes exhibit higher shear strengths when compared to natural soils. The shear strength parameters are given as per the test condition, drained or un-drained (ASTM D6528-07). Fly ashes exhibit a wide range of friction angles and apparent cohesion. The shear strength parameters of Indian fly ashes ranges between 30° - 45° and apparent cohesion ranges between 15-50 kPa (Sridharan et al. 2001d). For bottom ashes, Huang (1990) found that friction angle varies from 35° to 55° .

2.6.2 Compressibility

Compressibility characteristics of any particulate material, compression index C_c , and coefficient of volume change m_v , can be determined in the laboratory using one-dimensional consolidation test (IS: 2720-Part 15, 1986). The compression index of Indian fly ashes ranges between 0.105-0.219 and the coefficient of volume change, m_v ranges from 4.28×10^{-5} to 3.67×10^{-4} mm²/kN (Sridharan et al. 2001e). Compressibility characteristics of fly ashes depend on their initial dry unit weight, degree of saturation, self-hardening characteristics, the pozzolanic reactivity, and curing time.

2.6.3 Permeability

Coefficient of permeability of coal ashes is a function of grain size distribution, degree of compaction, and the pozzolanic property of the ashes. As bottom ash is coarser than fly ash coal, the bottom ashes are relatively more permeable than fly ashes.

The range of coefficient of permeability for Indian coal ashes is 8×10^{-6} - 7×10^{-3} (Sridharan et al. 2001e).

2.7 Review on interfacial shear tests and direct shear tests

Many research studies on the use of alternate material backfill material for retaining walls are available in the literature. To increase the stability of the slope or the wall, soil is being reinforced with geosynthetic materials. In a reinforced slope or wall, two kinds of failure - in shear and in pullout - are the common modes.

Recently, many research studies are being conducted on the interface properties of various geosynthetic materials with different soil types. Some studies were done with the addition of waste materials like tire chips to the soil to increase the strength of the soils (Aminaton et al. 2013; Attom 2006; Cabalar 2011; Edincliler et al. 2010; Foose et al. 1996; Ghazavi et al. 2005; Roa and Dutta 2006; Sheikh et al. 2013; Umashankar et al. 2014). Studies were carried out to know the feasibility to use the tire chips to improve the subgrade (Ayothiraman et al. 2011), in highway embankments (Bosscher et al. 1997), in backfills (Lee et al. 1999; Tweedie et al. 1998). Some studied the interaction of sand-tire chip mixtures with the geosynthetics (Umashankar and Prezzi 2010; Tatlisoz et al. 1998).

Tanchaisawat et al. (2010) studied the interaction between geogrid reinforcement and tire chip-sand mixtures. Two geogrids namely Saint-Gobain (geogrid A) and polyfelt (geogrid B) were selected as reinforcing materials. Tire chip-sand mixtures with different mix ratios 0:100, 30:70, 40:60, and 50:50 by weight were used as fill materials. The proportion 30:70 by weight was found to be most suitable mix ratio. The direct shear interaction coefficient and the efficiency values of geogrid B are found to be higher than that of geogrid A. The interaction coefficient of the geogrid B in pull out mode for the 30:70 mix ratio was found to be 0.71, and in direct shear mode it was found to be 0.92. They observed that the dry unit weight of tire chip-sand mixtures depended more on the sand content, and less on the water content.

Shear strength parameters of compacted fly ash-HDPE geomembrane interfaces have been studied (Adamska 2006). The study was done to find the interface shear strength parameters of fly ash with HDPE geomembrane. Geomembranes are generally used as a sealing material for landfills. Their study was carried out for a municipal landfill application in order to assure the leak proof. Geomembranes of different textures were used. Interface friction angle was found to be more for the textured geomembranes while adhesion was found to be more for smooth geomembranes. Textured geomembranes had peak and residual strength equal to twice to that of smooth geomembrane.

Naeini et al. (2012) had investigated for shear strength of silty sand-geogrid interface. The study was carried out to investigate the interface shear strength of sand reinforced by high-density polyethylene cogged geogrid, with variation in fines content from 0 to 45%. A set of large direct shear tests (30cm x 30cm x15 cm in length, width and height) were systematically conducted. The behavior of sand and silty sand reinforced with a special type of cogged geogrid was studied in terms of interfacial shear strength of the soil. The test results indicate that the reinforcement improved the shearing behavior of the sand and silty sand samples. The peak strength was attained at greater shear strain due to reinforcement and lowered the post-peak loss of strength of specimens with higher silt content, compared to the specimens with lower silt content. This indicates that the reinforcement and increasing the silt content tend to transform the shearing behavior of sand and silty sand specimens from a brittle to a ductile manner. The results also indicated that as the silt content increases up to 35%, the combined shear strength decreases. Further increase in the silt content made no significant change to the combined shear strength of the soil samples. They observed the increase in interface friction angle and apparent cohesion for reinforced sandy soils was greater than the reinforced silty sands.

Hillman and Stark (2001) studied the shear strength characteristics of PVC geomembrane-geosynthetic interfaces. They observed that the post peak strength loss was 25% for 100 to 400 kPa and there was even lesser loss in the case for 50 kPa.

Balunaini and Prezzi (2009) studied the interaction of ribbed-metal-strip reinforcement with tire shred-sand mixtures. Interaction between ribbed-metal-strip reinforcement and tire shred-sand mixtures prepared with various tire shred sizes (9.5 mm in nominal size, 50–100 mm in length, and 100–200 mm in length) and tire shred-to-sand mixing ratios (tire shred contents of 0, 12, 25, 100% by weight) were studied. The pullout capacities of ribbed metal strips embedded in tire shred-sand mixtures were obtained for three confining pressures (40, 65, and 90 kPa). The test results showed that the pullout capacity of ribbed metal strips embedded in tire shred-sand mixtures is much higher than that of ribbed metal strips embedded in samples prepared with only tire shreds. The pullout capacity of metal strip embedded in 25% tire chip-sand mixtures (by weight of tire chip in mixture) was higher than that of the same mixtures prepared with larger tire shred sizes (50–100 mm and 100–200 mm in length).

Anubhav and Basudhar (2010) studied soil-woven geotextile interface behavior using direct test results. Experiments were done in a direct shear apparatus to study the shear force-displacement behavior at the soil-geotextile interface using two differently textured woven geotextiles. A constitutive model had been presented for predicting both the pre-peak and post-peak interface behavior. The results were quite comparable with the experimental results. In the study, kalpi sand (a poorly graded having angular particles) resulted in a peak friction angle of 46° and with no apparent cohesion. The study was conducted in a shear box of size equal to 60 mm x 60 mm. The peak interface shear strength was significantly higher for coarse-textured geotextile with no openings, when compared to fine-textured geotextile with apparent opening size of 0.1 mm.

Athanasopoulos (1996) studied the geotextile reinforcement behavior on cohesive soils. He found that the inclusion of nonwoven geotextiles resulted in a significant strength increase of the wet cohesive soil. The inclusion of woven geotextiles, however, did not offer any strength increase. The resulted cohesion was around 40 kPa and friction angle was obtained as 14° .

Tuna and Altun (2012) carried out interface direct shear tests to investigate improvement in the mechanical behavior of granular soils when reinforced with geotextile inclusions. As expected, the interface friction angle of the reinforced sand was found to be lower than that of the unreinforced sand. No remarkable difference was seen in the shear strength of reinforced and unreinforced sands, but in reinforced sand, there was no post-peak loss of

strength, as seen in unreinforced sand. Unexpectedly, geotextile inclusions did not restrict the soil from dilating. If the geotextile content was increased in the test specimen, only then did the dilation of the sand decrease. The tests were conducted in a small shear box having the feasibility to include the geotextile at the interface. The friction angle values for the sand varied from 30° -to- 40° , whereas the apparent cohesion was quite high in the range 14 kPa-to-55 kPa. At the end of the results, it was concluded that the interface behavior depends on the combined effects of the surface properties and deformability of the geotextiles, and also on the index properties of the soil.

Foose et al. (1996) investigated the feasibility of using tire shreds to reinforce the sands. They found apparent friction angle as high as 67° . They concluded that the increase in tire shred content increases the strength.

Tatlisoiz et al. (1997) studied the interaction between geosynthetics and soil-tire chip mixtures. They investigated using two different soils (sand and silty sand). The shear strengths were found to be quite high for the geogrid reinforced silty sands.

2.8 Studies on fly ash and bottom ashes

Some studies were carried to know the possibility to use the fly ash and bottom ash mixtures in highway embankments (Kim et al.2005; Martin et al. 1990; Rai et al. 2010; Santos et al. 2011; Kim et al. 2009), in sub bases (Praveen and Shalendra 2008).

Some studies were done on fly ash and bottom ashes to know the geotechnical properties for using them in highway embankments (Kim et al. 2005). Representative samples of class-F fly and bottom ash were collected from two utility power plants in Indiana, USA, and tested for their mechanical properties, viz., compaction, permeability, strength, stiffness, and compressibility. Three mixtures of fly and bottom ash with different mixture ratios (i.e., 50, 75, and 100% fly ash content by weight) were prepared for testing. Test results indicated that ash mixtures compare favorably with conventional granular materials. The shear strength tests showed that the peak internal friction angle varies between 28° and 48° . This is fairly comparable with the internal friction angle of granular soils. This should be because of angularity of the particles in bottom ash and also depends on ash sources, test conditions like relative compaction, confining stress and fly ash content.

Huang (1990) studied the use of bottom ash in highway embankments, subgrade, and sub-bases. He investigated the shear strength of Indiana bottom ash and boiler slag compacted to different densities using direct shear testing. The reported friction angles varied in a wide range from 35 to 55° , depending on the density.

Chapter 3

Experimental work

The various properties of fly ash collected from Neyveli Thermal Power Plant and Ramagundam Thermal Power Plant were obtained by conducting suitable experiments. Fly ash from Neyveli plant was obtained from electrostatic precipitators and is designated as NFA, while the pond ash from Ramagundam is designated as RPA. The details on the raw materials used in the study are given in the following sections. The testing procedure is explained next.

3.1 Raw materials used

This study focuses on the interface shear characteristics of reinforcement with fly ash, and mixtures of fly ash and tire chips. Accordingly, the raw materials used in the study include fly ash from two sources (Neyveli fly ash and Ramagundam pond ash), tire chips, and geogrid. In addition, locally available sand was used for comparison of interface shear strength of proposed fill materials (fly ash and fly ash-tire chip mixtures) with the conventional granular fill (sand).

3.1.1 Neyveli fly ash (NFA)

As discussed in the earlier Chapters, Neyveli Power Plant produces two gradations of fly ash- coarse fly ash and fine fly ash. The fly ash used in the experiments was coarse fly ash, and Neyveli coarse fly ash is represented as NFA. Fig 3.1 shows the Neyveli coarse fly ash used for the present study. The ash was collected in plastic containers and transported to Indian Institute of Technology, Hyderabad (IITH), for further testing. The samples were stored in air-tight buckets during the testing program.



Fig 3.1 Neyveli coarse fly ash

3.1.2 Ramgundam pond ash (RPA)

Ash collected from the Ramagundam is a mixture of fine fly ash and bottom ash, collectively called as pond ash. Ash was collected from the pond where it was dumped through pipelines. The percentage of fly ash to that of bottom ash is generally 65:35 by volume. Ramagundam pond ash is represented as RPA hereafter. Fig 3.2(a) shows Ramagundam pond ash that was used in the present study. Ash was collected in plastic containers from the pond ash using back hoe, as shown in Fig 3.2(b), and shipped to IITH laboratory. Ash was then stored in air-tight buckets during the testing program.



Fig 3.2(a) Ramagundam pond ash



Fig 3.2(b) Collection of ash from the pond at Ramagundam

3.1.3 Sand

Sand used in the experiments was collected from locally available river bed. Fig 3.3 shows the photograph of sand used in the study.



Fig 3.3 River bed sand

3.1.4 Geogrid

Different types of geosynthetics are available in the market, viz., geogrids, geomembranes, geotextiles, geostraps, etc. Different geosynthetics have different applications, for example, geotextiles are used as a separator for different pavement layers, geogrids as a reinforcement

material, and geomembranes as a covering material. In this study, biaxial geogrids were used as the reinforcement material. Fig 3.4 shows the photograph of geogrid used in the experiments. Table 3.1 gives the properties of the geogrid.

Table 3.1: Properties of geo-grid

Property	Value
Mass per unit area	240 g/m ²
Maximum tensile strength	40 kN/m
Aperture size	31 mm x 31 mm

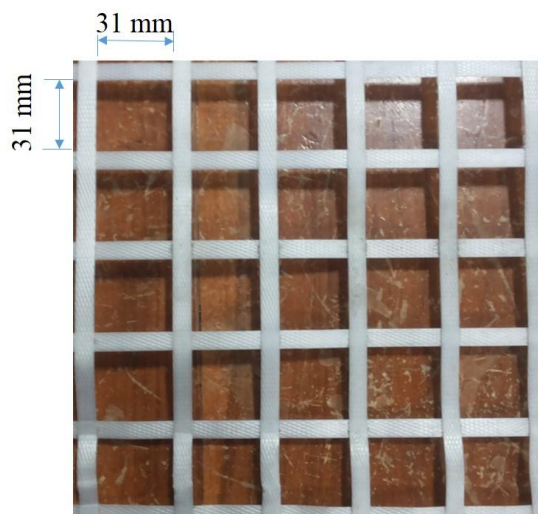


Fig 3.4 Photograph of geogrid specimen

3.1.5 Tire chips



Fig 3.5 Photograph of tire chips used in the study

Tire chips used for the study were collected from Entech Inc., located in White Pigeon, Michigan, USA. The nominal size of the tire chip is 9.5 mm, and Fig 3.5 shows the tire chips used in the study. The tire chips were characterized based on the attributes like length, width and thickness. However, the tire chips used in this study were found to be equidimensional (cubical) and in addition, no metallic or fiber reinforcements were present at their edges.

3.2 Experimental setup

Interface shear tests on geogrid and fly ash, and geogrid and fly ash-tire chip mixtures were performed using direct shear testing machine (Figure 3.6a). The Figure 3.6(a) shows the isometric view of the direct shear testing machine which is specially designed with a provision to include reinforcement material at the interface to perform the interfacial tests. The reinforcement is attached at the top of lower box using a clamping system. As in the case of direct shear testing, the lower box filled with sample is made to move in which the reinforcement material is fixed on the top. During shearing, the shear resistance will be offered by the interaction of soil and surface of geogrid ribs, interaction of soil particles within the openings of geogrid, and the passive resistance against the transverse ribs.



Fig 3.6(a) Photograph of interface shear testing machine

The shear box is comprised of two boxes connected with shear bolts as shown in Fig 3.6(b). The dimensions of lower and upper boxes were equal to 300 mm x 300 mm x100 mm (in length, width, and depth).

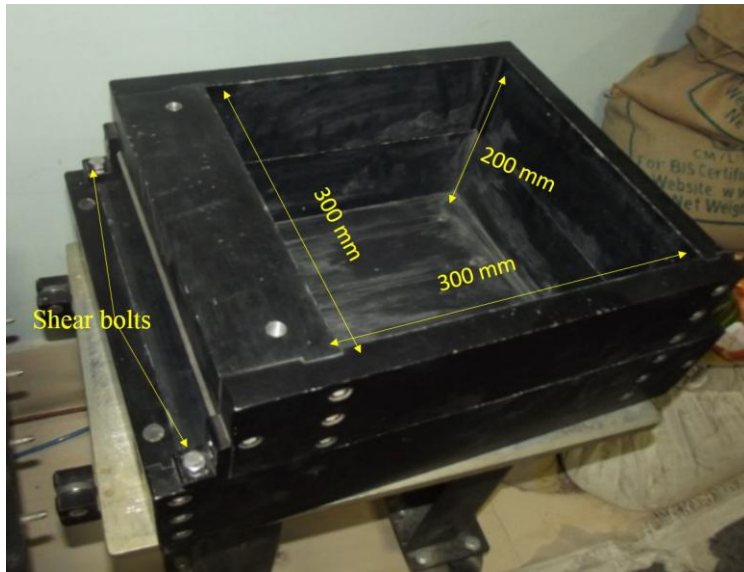


Fig 3.6(b) Photograph showing direct shear box

The other main parts of the machine are the load cells and Linear Variable Differential Transformer (LVDTs), as shown in Figures 3.6(c) and 3.6(d). Fig 3.6(c) shows the vertical load cell and vertical LVDT of maximum capacities 45 kN and 100 mm, respectively. While, Fig 3.6(d) shows the horizontal load cell and horizontal LVDT of capacities 45 kN and 100 mm.

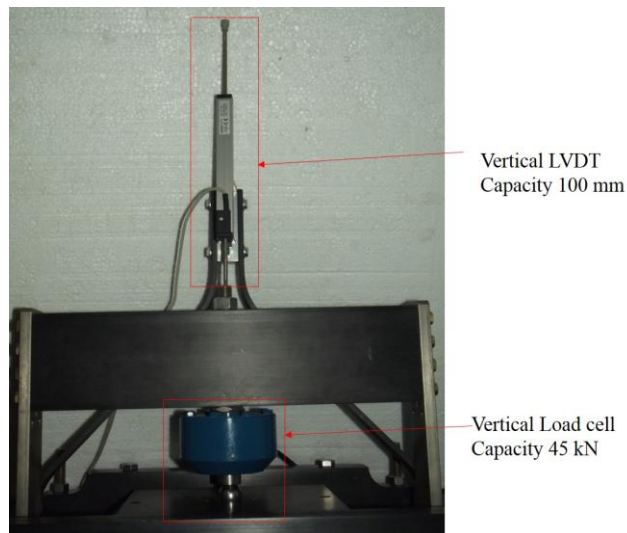


Fig 3.6(c) Vertical load cell and vertical LVDT

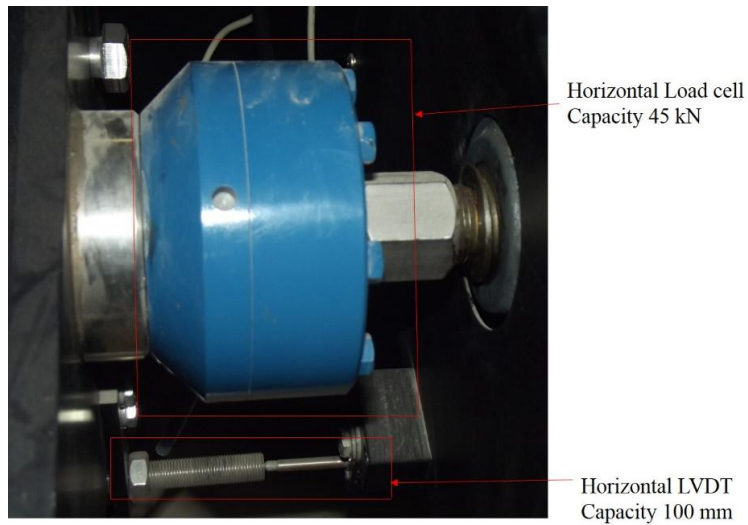


Fig 3.6(d) Horizontal load cell and horizontal LVDT

3.3 Tests conducted

Prior to conducting interfacial shear tests, characterization tests were done on the samples of Neyveli fly ash, Ramagundam pond ash, and sand to know their properties, like specific gravity, size and shape. The following sections explain the testing procedures.

3.3.1 Grain size analysis

Grain size analysis was done on the samples in accordance with the code prescribed by

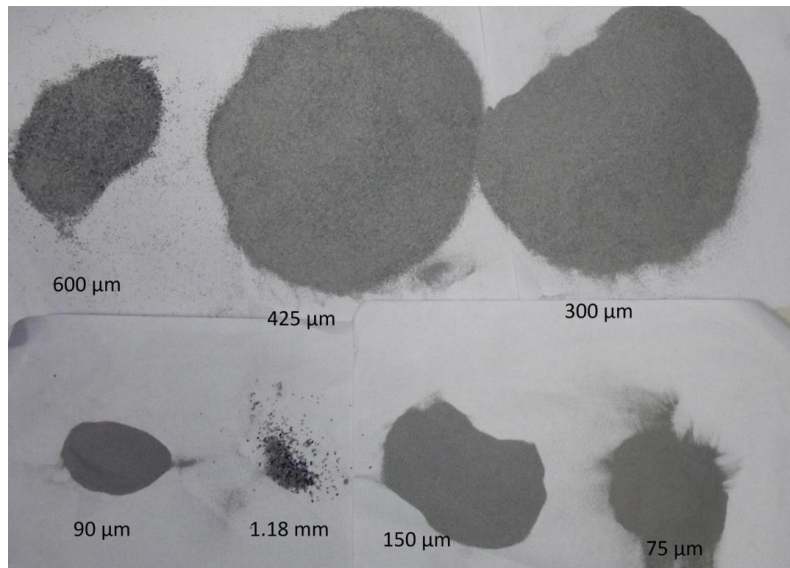


Fig 3.7 Retained NFA samples on the different sieves

the ASTM D422-63 (2007). A sample of mass equal to 1 kg was taken and was sieved through the recommended sieves placed in the ascending order of opening diameter with

sieve sizes of 0.075 mm, 0.09 mm, 0.15 mm, 0.3 mm, 0.425 mm, 0.6 mm, 1.18 mm, 2.36 mm, 4.75 mm with pan placed at the bottom. The entire sample was taken in 4.75 mm sieve, and the stacked sieves were shaken using a sieve shaker. Fig 3.7 shows the different gradation of particles of NFA. While Fig 3.8 shows the different gradation of particles of RPA. The percentage finer was calculated after the cumulative percentages of retained samples were measured.

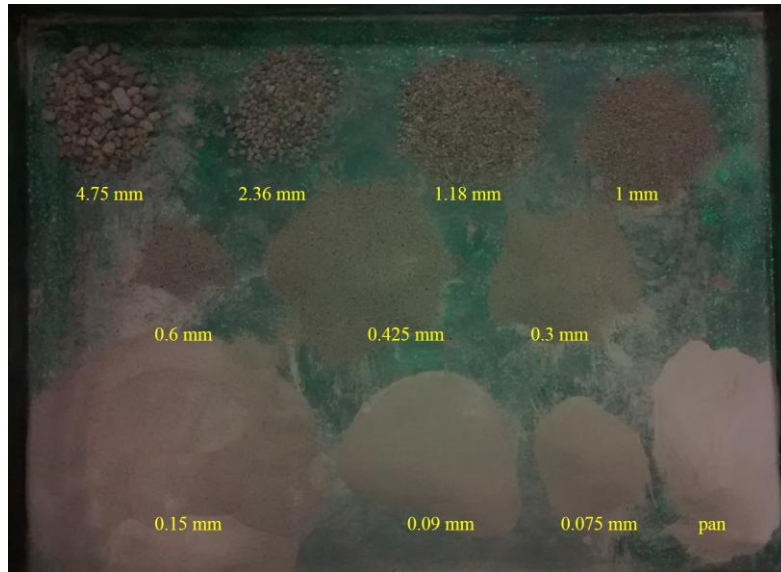


Fig 3.8 Retained RPA samples on different sieves

3.3.2 Specific gravity

The specific gravity of the samples was determined in accordance with ASTM D854-10. The test was done using density bottle apparatus. The empty weight of the density bottle with the lid was measured and noted down as W1. In the next step, some weight of sample was taken in the bottle and weighed with the lid, this weight was noted as W2. In the third step, the water was then filled in the remaining portion of the density bottle up to its neck. Now the bottle was connected to a vacuum pump through the lid at the top, and vacuum was gently applied to de-air any bubbles that are present in the sample, and the weight was noted down as W3. The contents of the bottle were then emptied, and was filled with filled with only water up to the neck. The measured weight was noted as W4.

Specific gravity of the sample was calculated using Equation 3.1

$$G = \frac{(W1 - W4) - (W2 - W3)}{(W4 - W1)} \quad (3.1)$$

The procedure was repeated for three trials and the average value for the specific gravity was noted down.

3.3.3 Standard Proctor compaction test

Standard Proctor compaction tests were performed on the samples in accordance with ASTM standard (ASTM D698 (2000)) to determine the maximum dry density (MDD) and the optimum moisture content (OMC). Water was added in regular percentages. The sample was prepared in three layers, and each layer was compacted with 25 blows per layer using a standard rammer of weight 2.5 kg. Fig 3.9 shows the sample in the mould after the first layer of compaction. After compaction of three layers, collar was removed and the sample surface at the top of the mold was leveled with a straight edge. The bulk unit weight of compacted sample was then calculated from the measured mass of compacted sample and the volume of the mold. The water content at the end of the compaction was obtained by taking three samples at three different levels of the mould. The dry unit weight was then calculated from the bulk unit weight and the water content. The compaction curve was plotted showing the variation of dry unit weight of compacted ash with the water content.



Fig 3.9 Photograph of compacted first layer of sample in 100mm-diameter mould

3.3.4 SEM analysis

Scanning Electron Microscopic (SEM) studies were conducted to analyze the shape of the elements of the elements. The analysis was done in Field Emission Scanning Electron Microscope (FESM) equipment by placing the sample on a gold coated stub and imaging was done using the software. The results of the SEM analysis represented in Chapter 4.

3.3.5 Chemical composition

Chemical composition of the ash samples were determined by doing X-ray Fluorescence (XRF) analysis. The results are represented in Chapter 4.

3.3.6 Direct shear and interfacial shear tests

After characterization studies were performed on the samples, the direct shear tests and interfacial tests were done following the ASTM D6528-07 and ASTM D5321, respectively. Firstly, the compaction energy needed to prepare the sample was decided. The compaction energy imparted to the ash sample per unit volume during Standard compaction test was equated with the energy to be imparted to the sample in the direct shear apparatus. The sample was prepared in three layers for direct shear tests, and in four layers for interfacial tests. Based on this, the number of blows per layer using Standard Proctor hammer was obtained as 430 in the case of direct shear tests, and 338 blows per layer in the case of interfacial tests. Fig 3.10 shows the preparation of compacted sample during direct shear and interfacial shear testing. Before placement of the loading plate on the compacted surface, the level surface was ensured using a level tube (Fig 3.11). Fig 3.12 and Fig 3.13 show the photographs during placement of geo-grid, and the clamped geogrid using bolts. After the compacted sample was prepared within the box, the box assembly was pushed in position to the direct shear/interface shear testing machine. It was ensured that the center of the box sits exactly under the vertical load cell. Once it was under the load cell, the load cell was moved down till it touched the ball on the loading plate. After that, bolt connections were done to ensure that the upper box did not move during shearing stage. Initially, the sample was consolidated under a given normal stress for few minutes to facilitate uniform application of required normal stress. Loading during consolidation was applied through the software. The shear phase was started after removing the shear bolts. During this phase, the lower box was moved as the upper box was held in initial position. All the shear tests and interfacial tests were done at displacement rate equal to 1mm/min with a maximum allowable horizontal displacement of 50 mm which is the extreme limit of movement of the lower box. Tests were repeated for different normal stresses to get a shear strength envelope by plotting the shear strength at each normal stress. Right after the preparation of the sample, it is weighed along with the box and weights were noted down and the bulk unit weights were calculated. Three samples at three different layers of the box were taken for determination of water content. After the water contents were obtained, the dry unit weights were calculated. The relative compaction needed to be achieved was cross checked with the targeted relative compaction.



Fig 3.10 Sample preparation in the direct shear box



Fig 3.11 Level tube used to ensure level compacted surface



Fig 3.12 Placing of geogrid on top of compacted sample in the lower shear box



Fig 3.13 Clamped geogrid

3.4 Fly ash- tire chips mixture

To prepare tire chips and fly ash mixtures for compaction testing, direct shear and interface shear testing, tire chips were mixed with ash with different percentage mixtures of tire chips. Three mixtures were prepared with 10%, 30%, 60% addition of tire chips (by weight of dry fly ash). Fig 3.14 shows the different steps followed in the compaction tests. The water was first added to fly ash to reach targeted water content and mixed uniformly. Tire chips were then and mixed further to obtain a uniform sample. The water content calculations were done based on the dry unit weight of fly ash. The results from compaction testing on mixtures are discussed in the Chapter 4.

During direct shear and interface shear tests, the same procedure was followed to prepare samples of fly ash and tire chips mixtures with different contents of tire chips. Mixtures were placed in shear box and compacted to required relative compaction. Procedure discussed in Section 3.3.6 was followed to conduct direct shear and interface tests on mixtures of fly ash and tire chips.



Fig 3.14 Preparation of fly ash and tire chip mixtures during standard Proctor compaction test

Chapter 4

Results and Discussions

Test procedures followed to conduct characterization studies, direct shear, and interface shear tests on sand, Neyveli fly ash and Ramagundam pond ash are detailed in Chapter 3. In this Chapter, the results from the testing program are presented. Characterization, direct shear, and interface shear tests conducted on each material used in the study are first presented. Finally, interface shear test results on geogrid and fly ash, and geogrid and mixtures of fly ash and tire chips are presented. The interaction coefficients of geogrid- fly ash and geogrid- fly ash-tire chip mixtures are proposed with respect to the shear strength properties of fly ash and fly ash-tire chip mixtures (obtained from direct shear testing).

4.1 Tests results on Sand

4.1.1 Grain-size distribution

Fig 4.1 shows the grain-size distribution curve for the sand used in the present study. Three samples of sand are tested to assess the variability in gradation.

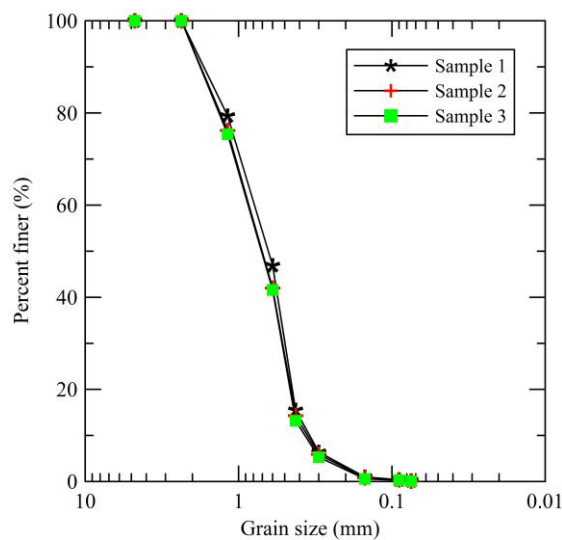


Fig 4.1 Grain-size distribution for sand

The coefficient of uniformity, C_u , and the coefficient of curvature, C_c , are calculated using the expressions

$$C_u = \frac{D_{60}}{D_{10}} \quad (4.1)$$

$$C_c = \frac{(D_{30})^2}{D_{60} \times D_{10}} \quad (4.2)$$

where, D_{10} , D_{30} and D_{60} correspond to the sizes for 10%, 30% and 60% finer than that size. The values of D_{10} , D_{30} and D_{60} are equal to 0.36mm, 0.48mm and 0.75mm, respectively. The average particle size (D_{50}) of sand is equal to 0.7mm. The gradation characteristics, C_u and C_c , are found to be equal to 2.125 and 0.735. Sand is classified as poorly-graded sand (SP).

4.1.2 Specific gravity

The average specific gravity obtained from three trials is reported as the specific gravity. The specific gravity of sand is obtained as 2.64. Typically, the specific gravity of sands ranges from 2.6-to-2.7.

4.1.3 Standard Proctor compaction test

Fig. 4.2 shows the variation of dry density vs. water content. The maximum dry density and the optimum moisture content of the sand are equal to 1.7 g/cc and 12%, respectively. As expected, the dry density at dry state was higher than that of the dry density corresponding to the optimum moisture content. The variation in dry density with water content was not significant. Due to no significant effect of water content on dry density, the samples were prepared at water content equal to 5% during direct shear and interfacial shear tests.

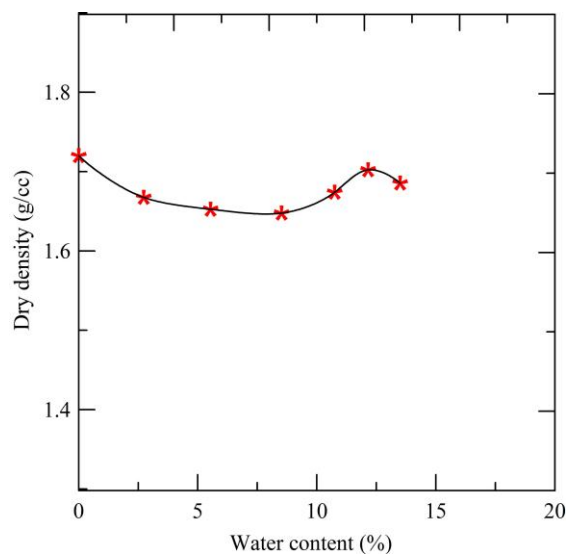


Fig 4.2 Compaction curve of sand

4.1.4 Morphology

SEM analysis was done to know the morphology of sand particles, and sand particles are found to be highly angular. Fig 4.3 shows the morphology of sand particles at magnification factors of 50x and 100x.

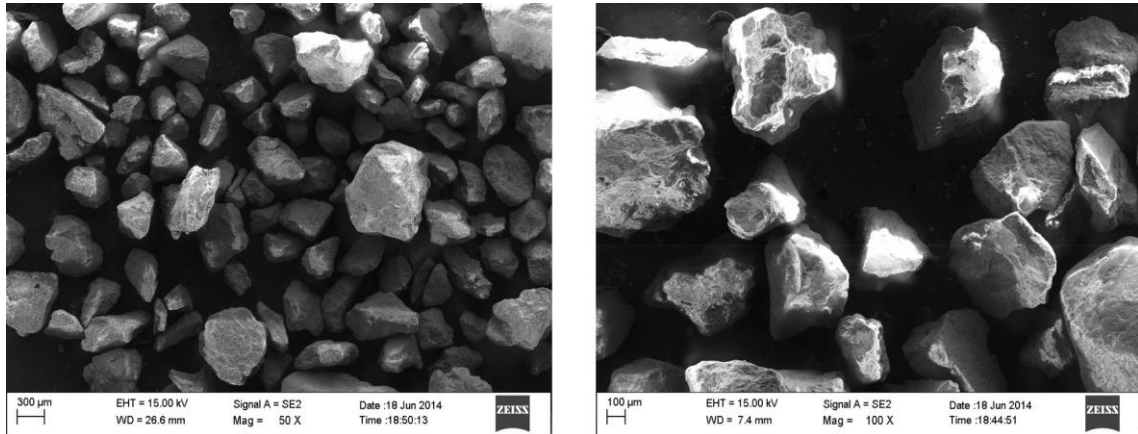


Fig 4.3 SEM images of sand at different magnifications

4.1.5 Results of direct shear and interfacial tests

The direct shear and interfacial shear tests were done on sand samples prepared with water content equal to 5%. The water content was fixed based on the targeted relative compaction equal to nearly 90%-to-95%. The tests were done at three different normal stresses- 50 kPa, 100 kPa and 150 kPa.

Prior to carrying out an extensive testing, repeatability in test results was checked by conducting direct shear tests on two identical sand samples under a normal stress of 100 kPa. Fig 4.4 shows the shear stress developed on the horizontal shear plane vs. the horizontal displacement of the lower box on two identical samples. The direct shear test results clearly show that the test results are repeatable. Further testing was then carried out.

Fig 4.5(a) shows the shear stress developed on the horizontal plane vs. the horizontal displacement of the box for sand samples subjected to normal stresses equal to 50 kPa, 100 kPa and 150 kPa (unreinforced case). Interface shear tests on sands with geogrid placed at the shearing plane are then performed. The test procedures involved in clamping the geogrid on top of the compacted sample in the lower box are detailed in Chapter 3. Fig. 4.5 (b) shows the shear stress developed on the horizontal plane vs. the horizontal displacement of the box with geogrid placed at the interface (reinforced case).

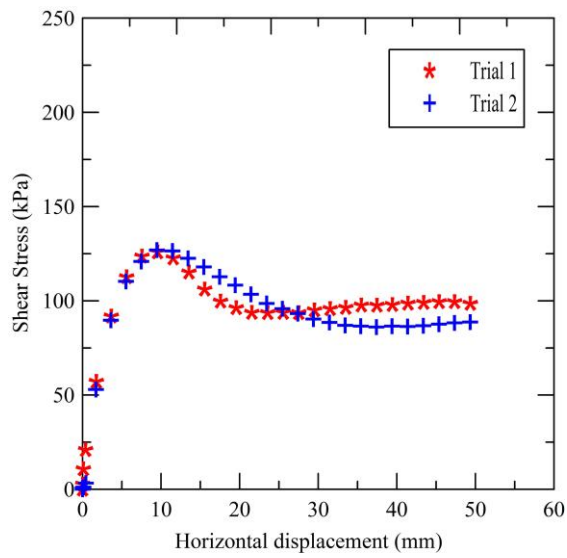
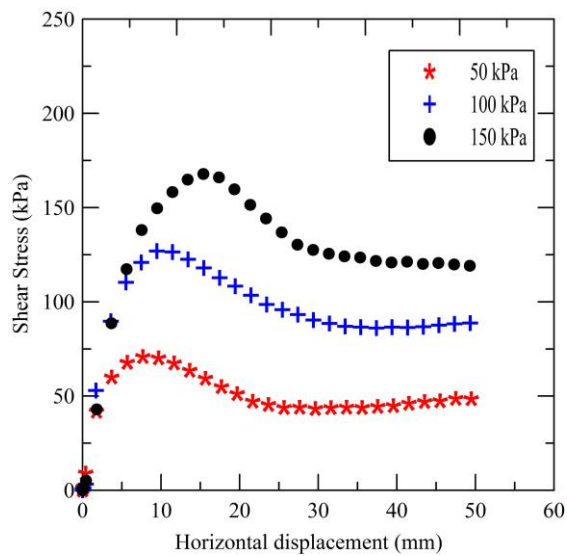
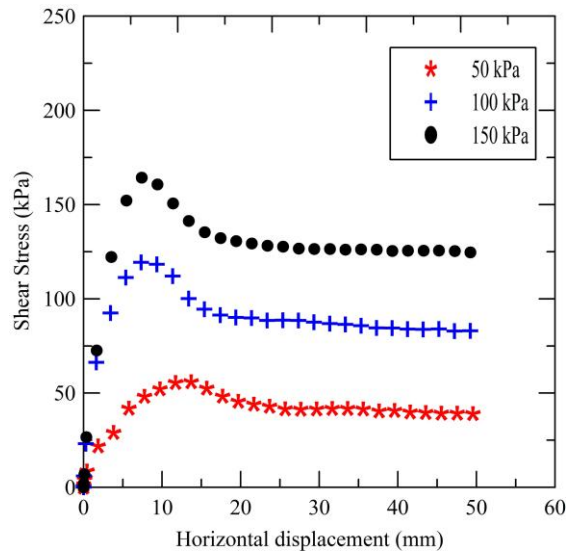


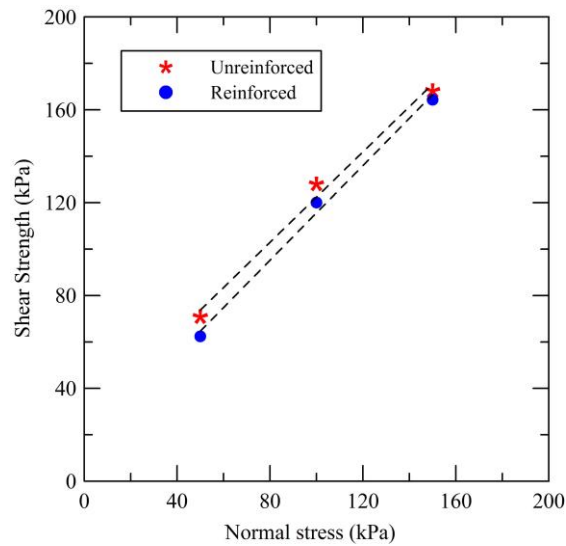
Fig 4.4 Shear stress vs. horizontal displacement of box on two identical sand samples at a normal stress equal to 100 kPa



(a)



(b)



(c)

Fig 4.5 (a) Shear stress vs. horizontal displacement of lower box for unreinforced sand, (b) Shear stress vs. horizontal displacement of lower box for reinforced sand, and (c) Peak shear strength envelopes for unreinforced and reinforced sand

Fig 4.5(c) shows the peak shear strength envelopes for unreinforced and reinforced cases. The shear strength envelope of sand sample is found to be slightly higher than that of interfacial shear strength envelope with geogrid placed at the shearing plane. This is because the frictional resistance between the geogrid material and sand is lower than that of frictional resistance between sand particles. It may be noted that the interfacial shear is mainly offered by the interaction of soil and surface of geogrid ribs, interaction of soil particles in

the openings of geogrid, and the passive resistance against the transverse ribs. The peak states are observed corresponding to horizontal displacement of the lower box ranging from 8 mm-to-17 mm in unreinforced case, and 8mm-to-11 mm in reinforced case.

The efficiency of geogrid was studied with respect to both cohesion and friction angle. For any reinforcement material, the aperture ratio plays a crucial role in offering the strength to the sample. Aperture ratio is defined as the ratio of aperture size of geosynthetic to the average soil particle size. The interfacial efficiency of geosynthetic with respect to cohesion is given as,

$$E_c = \frac{C_a}{C} \quad (4.3)$$

where, C_a is the adhesion between the geosynthetic and the soil particles, and C is the apparent cohesion between the soil particles. In a similar way, interfacial efficiency of geosynthetic with respect to friction angle is given as

$$E_\phi = \frac{\tan \delta}{\tan \phi} \quad (4.4)$$

where, δ implies the soil-geosynthetic interface friction, while ϕ is the friction angle of soil. The interaction efficiency of the geogrid with the raw materials used in the study (Neyveli fly ash, Ramagundam pond ash, and sand (are calculated and presented in Section 4.4.

4.2 Test results on Neyveli fly ash

4.2.1 Grain-size distribution

Fig 4.6 shows the grain-size distribution of NFA. Three trials are conducted on three different samples to check the variability in gradation.

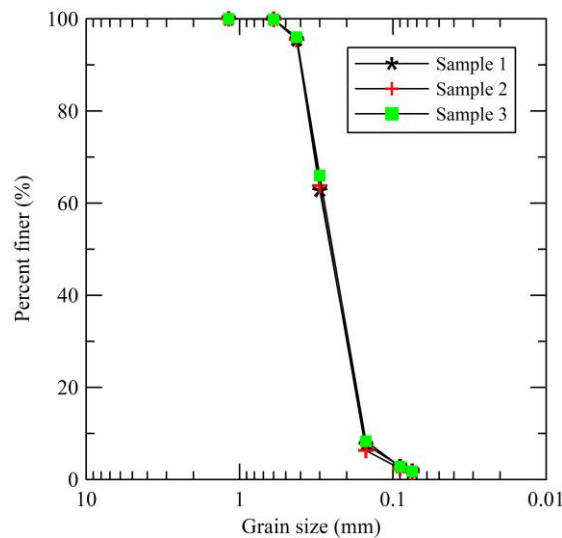


Fig 4.6 Grain-size distribution for NFA

C_u and C_c values are calculated using values of D_{10} , D_{30} and D_{60} , and are found to be equal to 1.76 and 0.78, respectively. The average particle size, D_{50} , of NFA is equal to 0.25. As per the classification, half of the coarse fraction is smaller than 4.75 mm and does not meet the criteria for SW as $C_u < 6$ and C_c does not lie in the range of 1 and 3. Hence, NFA is classified as poorly-graded sand type material. It is represented as SP. Neyveli coarse fly ash particles have size similar to the size of bottom ash particles. Indian bottom ashes are generally classified as SP or as SP-SMN with no plastic fines (Sridharan et al. 2001a).

4.2.2 Specific gravity

The average specific from the three trials is found to be equal to 2.54. The specific gravity of Indian fly ashes having bottom ash sized particles generally lies in the range 1.64 -to- 2.66 (Sridharan et al. 2001a). The higher specific gravity could be due to presence of higher content of iron oxide (Fe_2O_3).

4.2.3 Standard Proctor compaction test

The results of the standard Proctor compaction test on NFA are discussed below. Fig 4.7 shows the compaction curve of NFA.

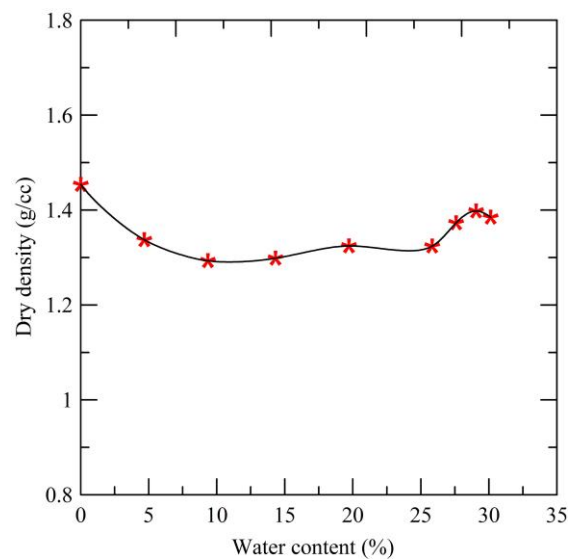


Fig 4.7 Compaction curve of NFA

The maximum dry density and optimum moisture content from the compaction testing are found to be equal to 1.4 g/cc and 29%, respectively. The range of dry density reported in the literature varies between 0.88-1.51 g/cc, and optimum moisture content varies from 21.3-58.1% (Sridharan et al. 2001f). The trend obtained from compaction testing in the present study is similar to that of granular soils. It is dumb-bell shaped curve. Similar to granular

soils, the effect of water content on compacted dry density was not significant. The compacted dry density of tested fly ash lies in the narrow range of 1.3 - 1.4 g/cc. For the direct shear and interfacial testing, samples were prepared with 20% water addition in order to achieve 95% relative compaction.

4.2.4 Morphology

SEM analysis was done to study the morphology of the NFA particles. The study was carried out at different magnifications. The SEM images indicate that the particles are angular in shape which is expected for coarse-grained soil particles (Fig 4.8).

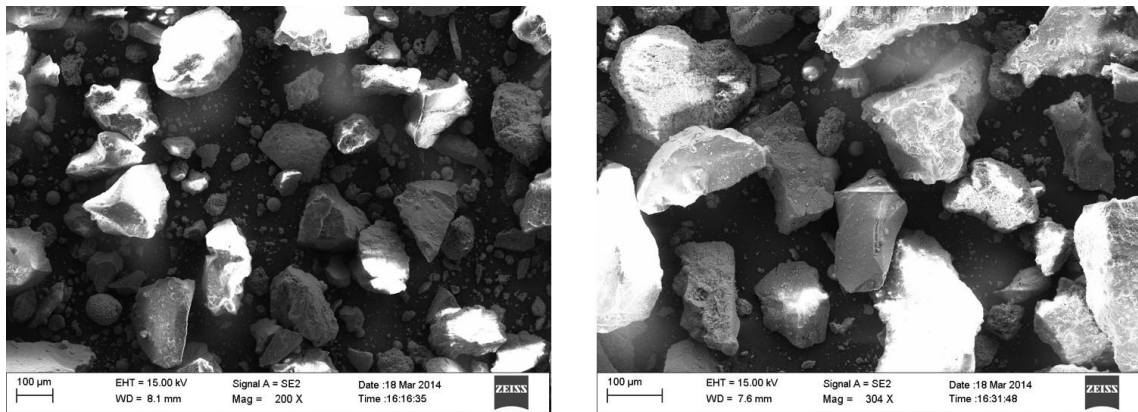


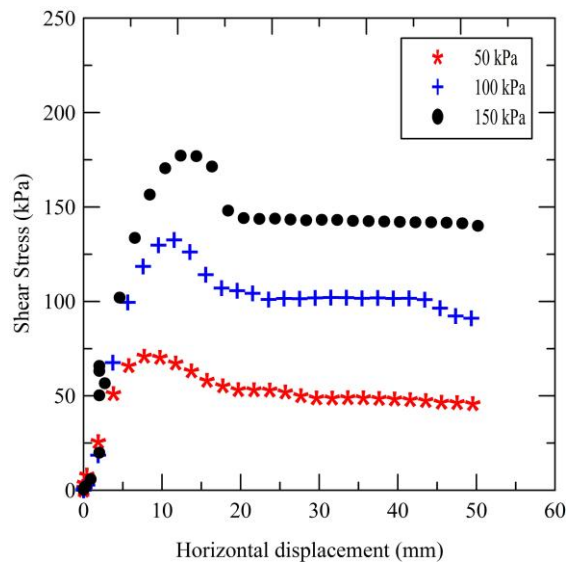
Fig 4.8 SEM analysis of NFA at different magnification

4.2.5 Chemical composition

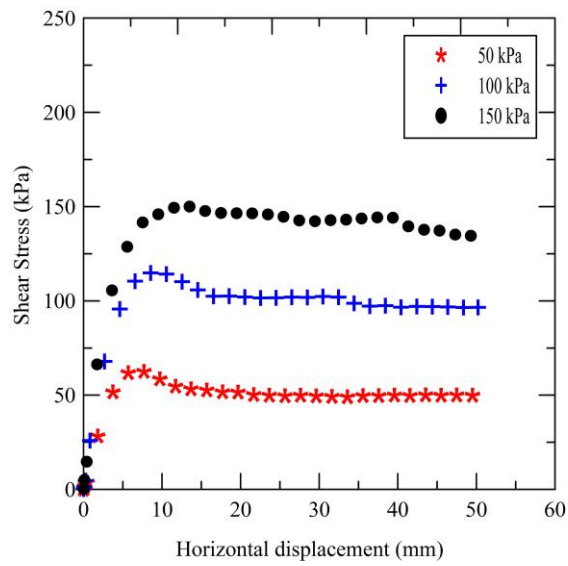
XRF analysis was done using XRF spectrometer which gives the chemical composition of the fly ash when the sample is analyzed. The results indicate the percentages of various chemical compounds present in the material in terms of weight. The resulting chemical composition of NFA shows 62% silica, 21% alumina, 4.9% CaO, 6% Fe₂O₃, and oxides of Na, Ti, S, etc., present in minor quantities. This fly ash is classified as Class-F fly ash in accordance with ASTM C618.

4.2.6 Direct shear tests and interfacial tests

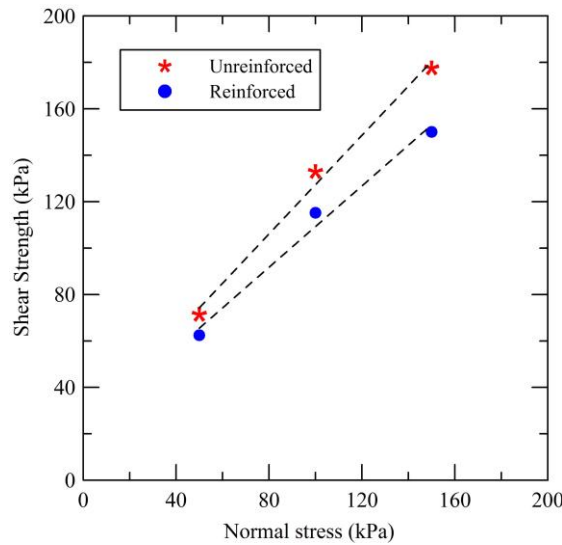
As discussed in the Chapter 3, the tests were conducted following the procedures suggested by the codes mentioned in the Section 3.3.6. The direct shear and interface tests are conducted on compacted NFA samples, and geogrid reinforced NFA samples. The same normal stresses (equal to 50 kPa, 100 kPa and 150 kPa) are applied on the sample. Figures 4.9(a), 4.9(b) and 4.9(c) show the results obtained from the testing.



(a)



(b)



(c)

Fig 4.9 Shear stress vs. horizontal displacement of the box for (a) unreinforced NFA, (b) Shear stress vs. horizontal displacement of lower box with geogrid reinforced NFA, and (c) Peak shear strength envelopes for unreinforced and reinforced NFA

Post peak reduction in shear stress is less in the case of geogrid reinforced NFA compared to that of NFA alone (Figs 4.9 (a) and (b)). Fig 4.9(c) shows the failure envelopes for both reinforced and unreinforced cases. It is observed that the horizontal displacement of the box to reach the peak state is higher in the case of unreinforced sample than that of reinforced case. The peak states were reached at horizontal displacement of the lower box ranging from 8 mm-to-14 mm in the unreinforced case, and at a displacement of 7 mm-to-14 mm in reinforced case. In most of the cases, the displacement at the point of failure was lesser in the case of reinforced sample when compared to the case of unreinforced sample. The direct shear parameters, the friction angle ϕ and the apparent cohesion, c , of NFA are given in Table 4.1. The interfacial shear parameters, δ and C_a , are also calculated from the test results (Table 4.1).

4.3 Ramagundam pond ash

Basic characterization studies are performed on Ramagundam pond ash prior to direct shear and interfacial tests. The results are presented in the following sections.

4.3.1 Grain-size analysis

Grain-size analysis was done on RPA as per the procedure outlined in Section 3.3.3.1. Three trials were done with three different samples, and the results are presented in Fig 4.10.

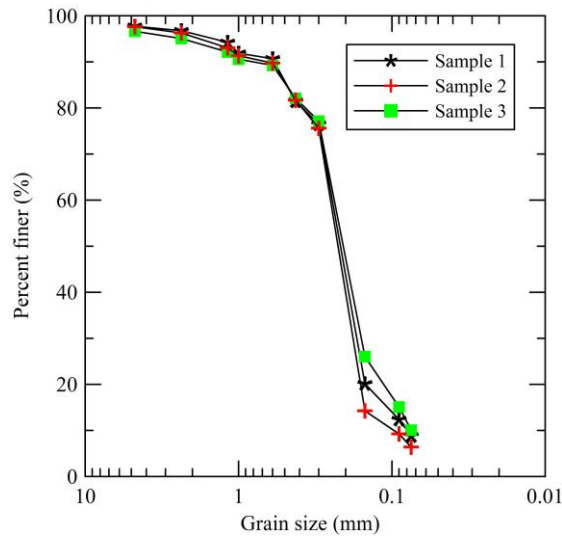


Fig 4.10 Grain-size distribution of RPA

The average values of D_{10} , D_{30} and D_{60} are equal to 0.08mm, 0.17mm, and 0.25mm, respectively, from the three trials. The average particle size, D_{50} , of NFA is equal to 0.2mm. The coefficient of uniformity and the coefficient of curvature are calculated and found to be equal to 3.06 and 1.47, respectively. This indicates that the used RPA is poorly-graded sand type with non-plastic fines.

4.3.2 Specific gravity

The average specific gravity from the three trials is found to be equal to 2.01. The typical range of specific gravity for Indian pond ashes is 1.64-2.66 (Sridharan et al. 2001a).

4.3.3 Standard Proctor compaction test

From Fig 4.11, the maximum dry density and the optimum moisture content for the RPA are

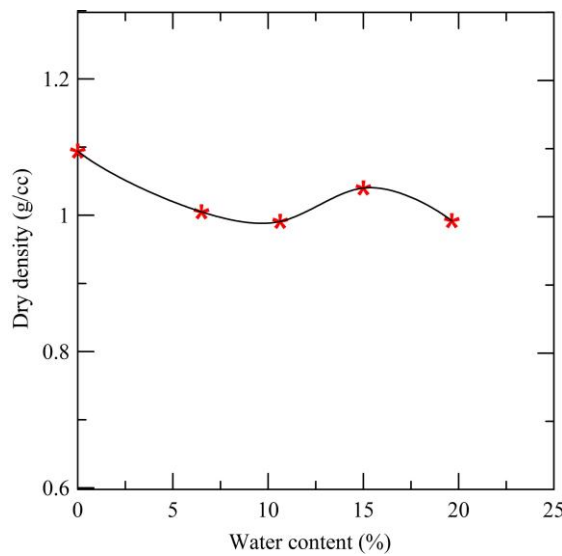


Fig 4.11 Compaction curve of RPA

equal to 1.04 g/cc and 15%, respectively. The dumb-bell shape of RPA signifies that the sample is granular. The range of the maximum dry density for pond ashes is 0.9-1.72 g/cc and the OMC ranges between 14.2%- 36.8% (Sridharan et al. 2001f). The variation in the dry densities with increase in water content is not significant. Hence, for the direct shear and interfacial tests, samples are prepared to the maximum dry density with water content near to OMC.

4.3.4 Morphology

Morphology of the RPA particles were studied under the SEM, and Fig 4.12 shows the SEM images produced at different magnifications. Fig 4.12 indicates that most of the particles of RPA are spherical in shape with some angular particles. This is expected as the pond ash used is a mixture of fly ash and bottom ash.

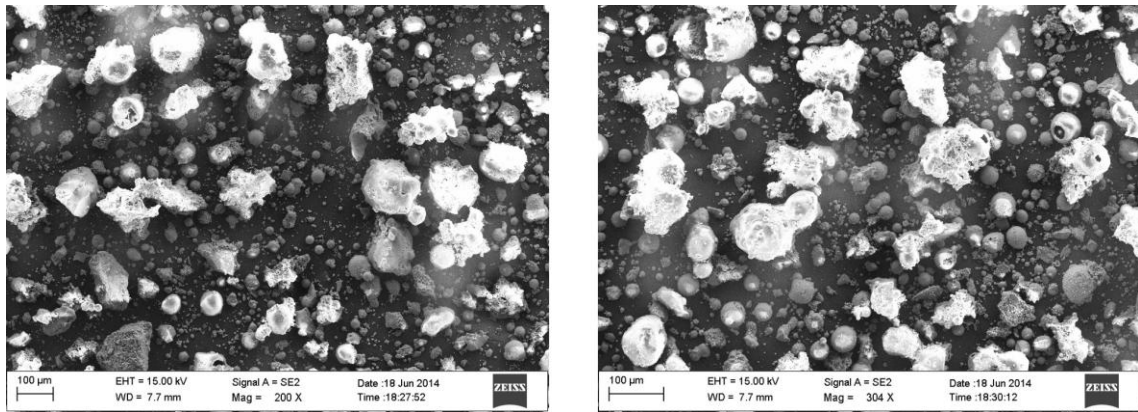


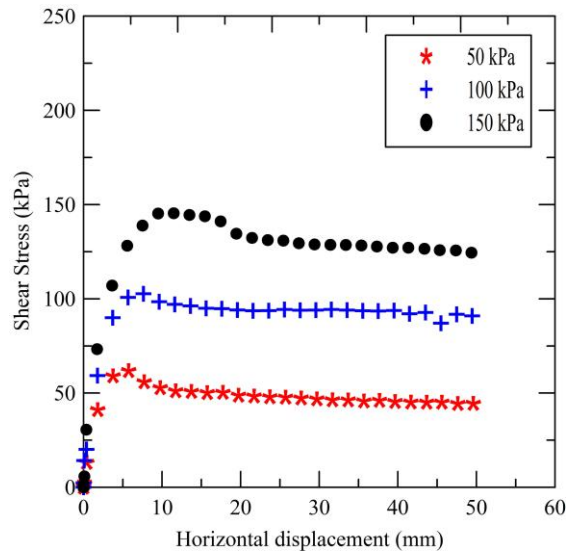
Fig 4.12 SEM images of RPA at different magnifications

4.3.5 Chemical composition

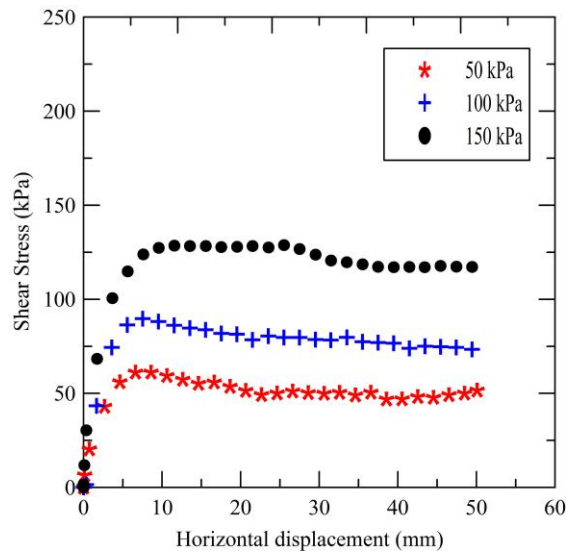
The chemical composition of the pond ash was determined by XRF analysis, and chemical composition was found to be a mixture of 59% silica, 19.5 % alumina, 3.1% CaO and 15.3% Fe₂O₃, and oxides of Mg, Ti, S, Na and K in minor quantities by weight. In accordance with ASTM C618, RPA is classified as Class-F fly ash.

4.3.4 Direct shear and interfacial tests

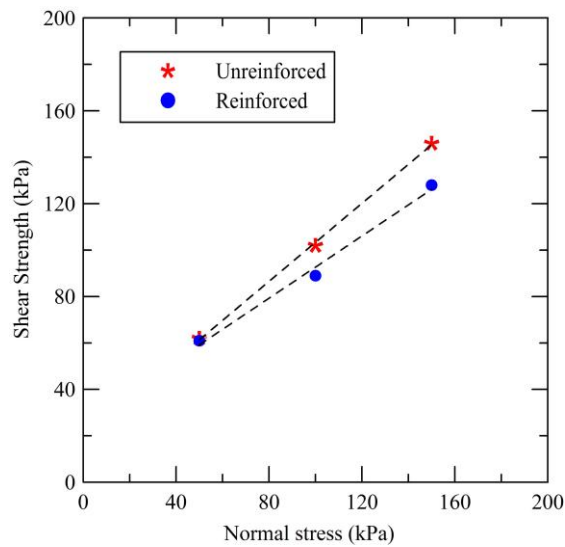
Direct shear and interfacial tests were done on RPA on samples compacted to a targeted relative compaction. The compacted density of samples prepared was nearly equal to the maximum dry density. Figures 4.13(a) and (b) shows the variation of shear stress vs. horizontal displacement of the lower box for unreinforced and reinforced samples. While Fig 4.13(c) shows the shear strength envelopes for both reinforced and unreinforced cases.



(a)



(b)



(c)

Fig 4.13(a) Shear stress vs. horizontal displacement of lower box for unreinforced RPA, (b) Shear stress vs. horizontal displacement of lower box for reinforced RPA, and (c) Peak shear strength envelopes of reinforced and unreinforced RPA

From 4.13(a) and (b), it is observed that the post peak loss in shear stress is less for reinforced case compared to that of unreinforced case. The shear strength envelope for RPA is higher than that of reinforced RPA. At lower normal stresses both the reinforced and unreinforced samples give same strengths. The peak states are achieved for horizontal displacement of box ranging from 5 mm-to-11 mm in unreinforced case, and 7 mm-to-12 mm in reinforced case.

4.4 Comparison of the interface shear strengths of NFA, Sand, and RPA with geogrid

Fig 4.14 shows the interfacial shear strengths of NFA, sand, and RPA. Fig 4.14 indicates that the NFA possess higher shear strength than that of sand and RPA. The shear strengths represented correspond to that at the peak state. The higher values of the shear strength of NFA can be attributed to the presence of angular particles.

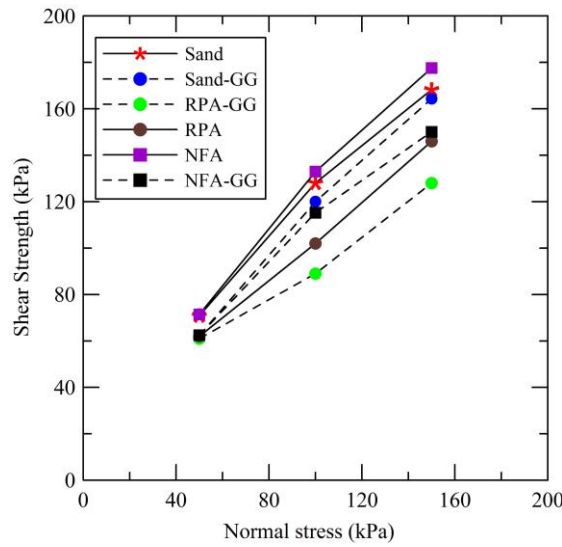


Fig 4.14 Comparison of shear strength envelopes of reinforced and unreinforced samples prepared with NFA, RPA and sand

The interfacial shear strength is lesser than that of shear strength of unreinforced samples. The interfacial shear strength is compared to the direct shear strength of the sample, and is represented in the terms of efficiencies as discussed in the Section 4.1.5. The efficiencies of the samples with respect to cohesion and with respect to friction are given in Table 4.1.

Table 4.1: Efficiency of geogrid with respect to cohesion and friction for NFA, sand and RPA

Raw material	C_a (kPa)	δ ($^\circ$)	C (kPa)	Φ ($^\circ$)	E_c (%)	E_ϕ (%)
Sand	13.6	45.5	25	44.2	54	112
NFA	21.7	41.2	21.1	46.2	102	82.5
RPA	25.6	33.8	19.3	40	130	79.7

E_c and E_ϕ give the percentage of strengths attained by the samples with respect to cohesion and friction. E_c values of NFA and RPA indicates that the adhesion is higher between the ash particles and geogrid reinforcement than that of the apparent cohesion between ash particles alone. However, adhesion between geogrid and sand is lower than the apparent cohesion of sand. E_ϕ value of sand indicates that the interface friction between the sand and geogrid is higher than that of ash samples and geogrid. The efficiencies shows that the geogrids are useful in attaining higher strengths along with the various benefits of reinforcing the fill material, like reduction in the deformation, increase in the tensile strength, etc. Tuna and Altun (2012) also reported greater shear strengths and interfacial

shear strengths. They reported adhesion values ranging between 13-55 kPa and the interface friction angle ranging from 32° and 40°.

Interface interaction coefficient, R_i , can be calculated based on the shear strength of reinforced soil and shear strength of unreinforced soil as (Tanchaisawat et al.2010),

$$R_i = \frac{(\sigma \tan \delta + c_a)}{(\sigma \tan \Phi + c)} \quad (4.5)$$

Where, σ is the normal stress, C_a is the adhesion between the soil and geogrid, C is the cohesion between soil to soil, δ is the geogrid-soil interface friction angle, ϕ is the friction angle of soil. Table 4.2 gives the interaction coefficient of geogrid for all the samples considered in the study. R_i signifies the fraction of interface shear strength with respect to shear strength of soil. Table 4.2 indicates that interface shear strength between fly ash and geogrid range from 0.87-0.90. This is only slightly lower than interface shear strength between sand and geogrid (R_i equal to 0.92).

Table 4.2: Interaction coefficient of geogrid

	For NFA	For sand	For RPA
Normal stress (kPa)	Ri at peak state	Ri at peak state	Ri at peak state
50	0.89	0.97	0.96
100	0.87	0.94	0.89
150	0.86	0.87	0.86
Average Ri	0.87	0.92	0.90

4.5 Tire chips

Grain-size analysis was performed on tire chips and Fig 4.15 shows the grain-size distribution of tire chips. The specific gravity of the tire chips was found to be equal to 1.16. Three samples of tire chips were sieved to assess the variability in the gradation. The values of C_u and C_c are calculated from D_{10} , D_{30} and D_{60} sizes and are found to be equal to 1.16 and 1.0. Tire chips can be classified poorly-graded gravel type (GP) as $C_u < 4$ and C_c is not in the range of 1 to 3.

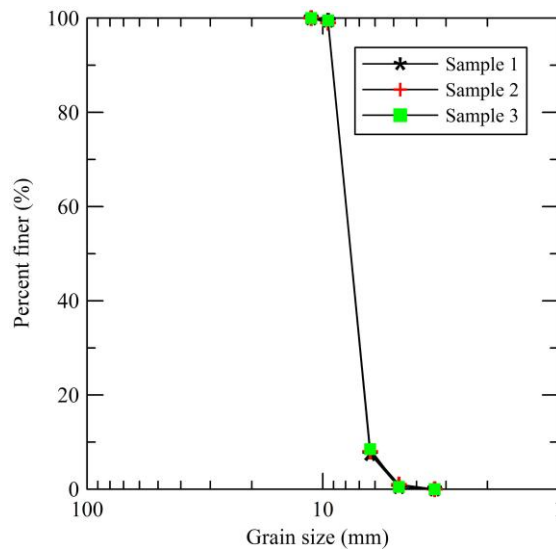


Fig 4.15 Grain size distribution for tire chips

4.6 Tire chips and NFA, RPA mixtures

Many research studies are available on the shear strength of sand and tire chips. In this study, tire chips were mixed with ash in different proportions (10%, 30% and 60%, by dry weight of fly ash). Direct shear tests and interface tests were carried out on the mixtures of fly ash and tire chips. Prior to shear tests, compaction tests were done on fly ash (either NFA or RPA) and tire chips. The water content calculations were made with respect to the dry weight of fly ash but not with respect to solids (fly ash and tire chips). The optimum moisture content values ranges between 22.5 to 29% for different tire chip mixtures of NFA and the maximum dry density varied between 1.15-1.4 g/cc. whereas for RPA, the optimum moisture content varied between 15-37% for different tire chip mixtures and maximum dry density varied between 0.91-1.09 g/cc. Fig 4.16(a) and Fig 4.16(b) gives the compaction curves for the tire chip mixed NFA and RPA.

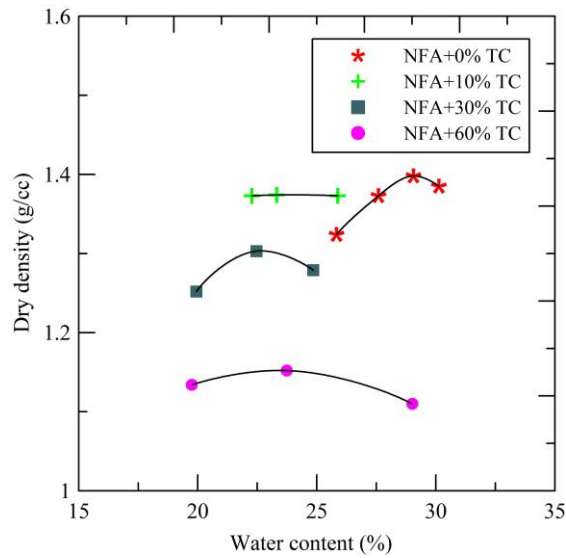


Fig 4.16(a) Compaction curves of mixtures with different percentage of tire chips mixed with NFA

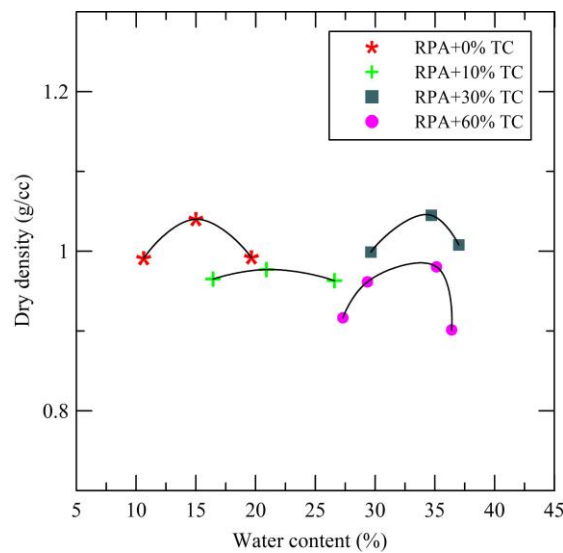
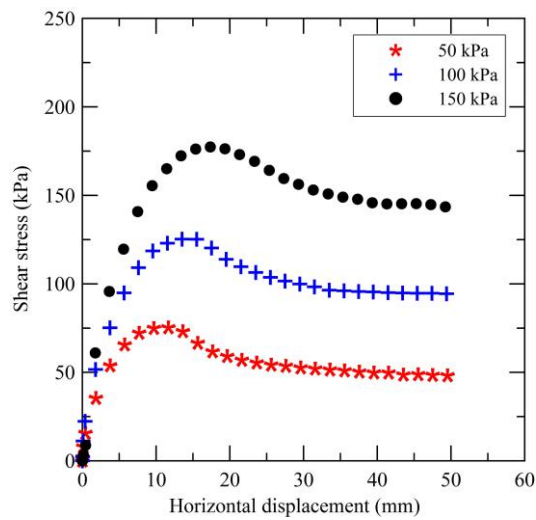


Fig 4.16(b) Compaction curves of mixtures with different percentage of tire chips mixed with RPA

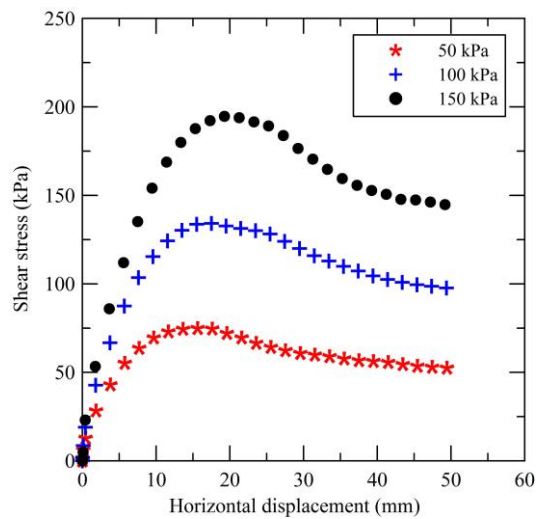
As expected the maximum dry density kept on decreasing with the addition of tire chips to NFA, whereas in the case of RPA the 30% addition of tire chips showed a maximum dry density equal to that of maximum dry density for only RPA. This could be because of the water insensitivity exhibited by the pond ash and the maximum packing of materials as the mixture has optimum amount of tire chips, bottom ash, fine fly ash and the water.

For direct shear and interface testing on the mixture of tire chips and ash samples, the water contents were selected in such a way that relative compaction equal to 90-95% relative compaction can be achieved. From Fig 4.17(a), (b) and (c), it is observed that the peak shear

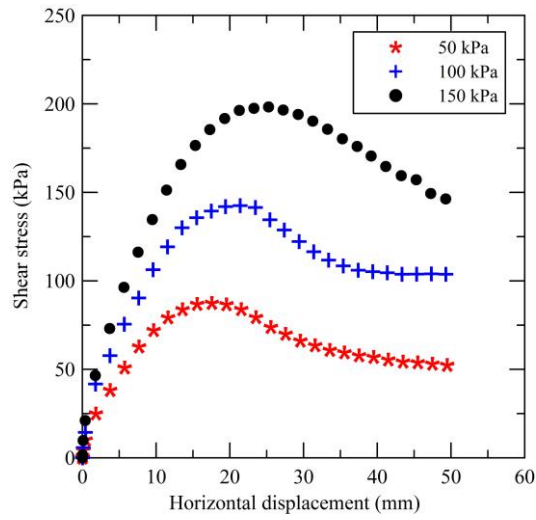
stress is reached at horizontal displacement of the box in the range of 13mm-17mm, 16mm-20mm, and 19mm-25mm, respectively, for 10%, 30% and 60% addition of tire chips respectively at normal stresses of 50 kPa, 100 kPa and 150 kPa. Higher the tire chips percentage, higher is the horizontal displacement for the failure. Fig 4.17(d) shows that the addition of 60% tire chips gives higher shear strength when compared to other percentage additions. However, the shear strength of 30% addition is nearly the same as that of 60% addition of tire chips.



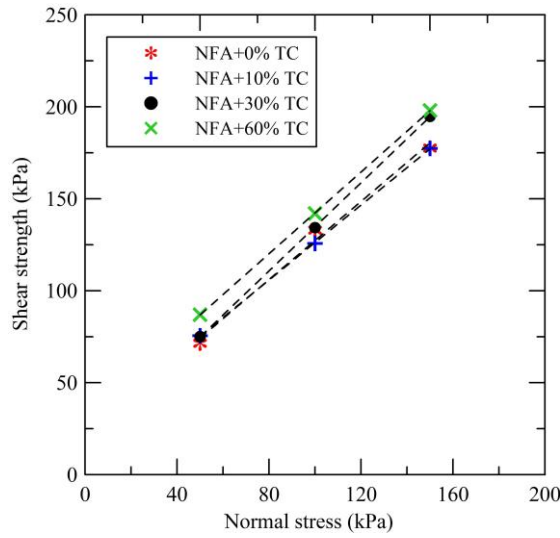
(a)



(b)



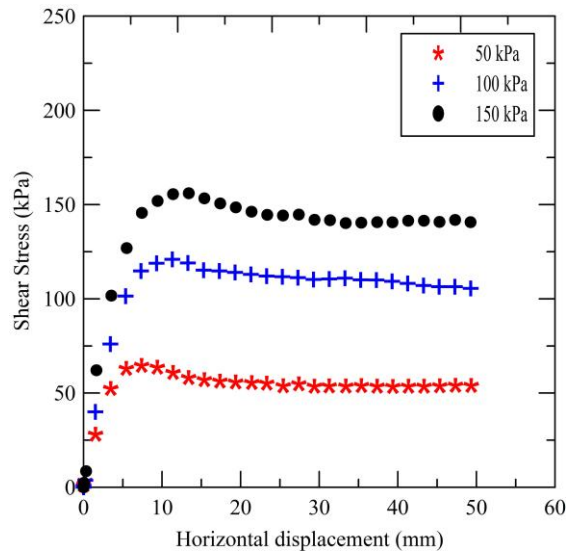
(c)



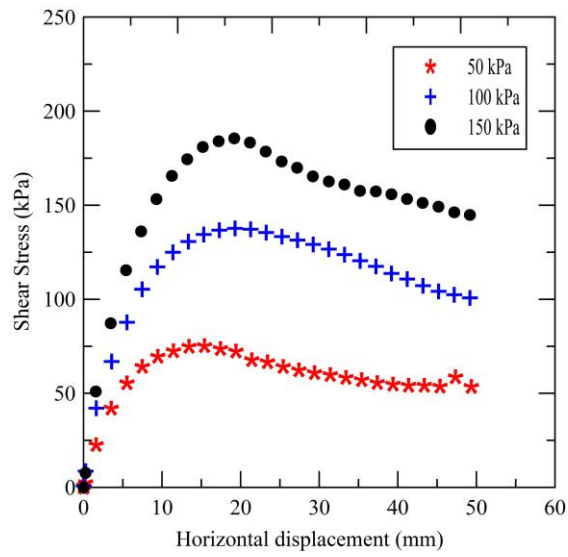
(d)

Fig 4.17(a) Shear stress vs. horizontal displacement of box for unreinforced NFA with 10% tire chips addition (b) Shear stress vs. horizontal displacement of box for unreinforced NFA with 30% tire chips addition (c) Shear stress vs. horizontal displacement of box for unreinforced NFA with 60% tire chips addition (d) Peak shear strength envelopes with different amounts of tire chips and NFA

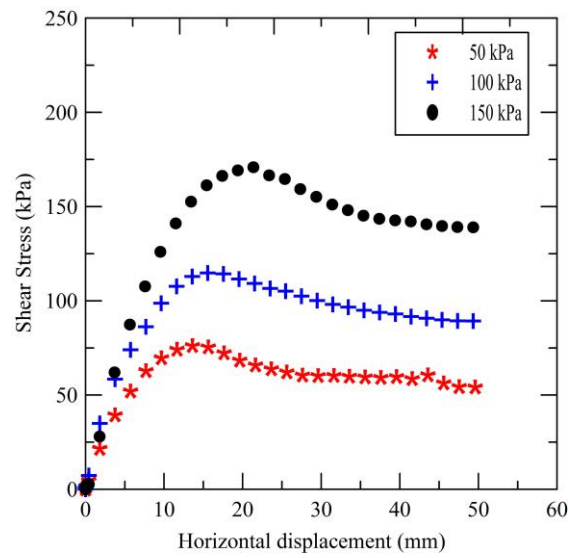
The following figures are the results for the interfacial shear tests on tire chip mixed NFA.



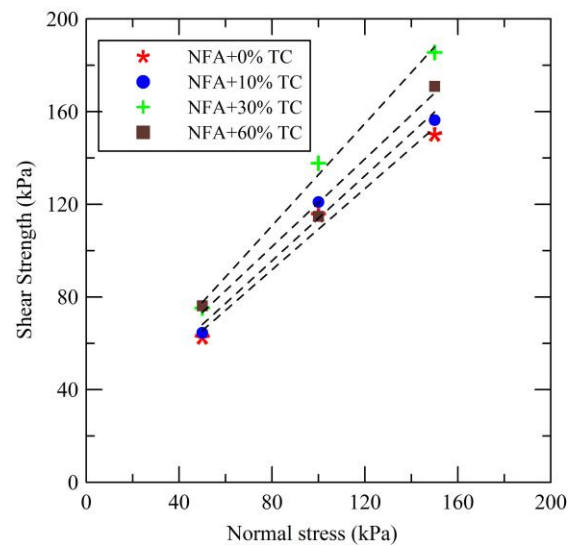
(a)



(b)



(c)



(d)

Fig 4.18(a) Shear stress vs. horizontal displacement of box for reinforced NFA with 10% tire chips addition (b) Shear stress vs. horizontal displacement of box for reinforced NFA with 30% tire chips addition (c) Shear stress vs. horizontal displacement of box for reinforced NFA with 60% tire chips addition (d) Peak interface shear strength envelopes with different amounts of tire chips and NFA

The interfacial shear strength increased with the addition of tire chips to the NFA. Figure 4.18(d) clearly shows that the interface shear strength envelopes with 30% and 60% tire chips are higher than fly ash alone and 10% tire chips and 0% tire chips. Table 4.3 gives the direct shear and interface shear parameters for different percentages of tire chips added to

NFA along with the efficiency of geogrid with respect to cohesion and friction. Figs 4.18(a), (b), and (c) show that the displacement needed to reach the peak state increases with the addition of tire chips. Efficiency of geogrid with respect to cohesion and friction are calculated using the Eq. 4.3 and Eq. 4.4, respectively. The ranges of horizontal displacements to reach the failure state (peak state) are equal to 6-11 mm, 12-20 mm and 13-22 mm for 10%, 30% and 60%, respectively. The higher the content of tire chips, the higher is the horizontal displacement to reach the peak state. This could be an advantage in delaying the sudden sliding failures in the earthen fills. The post peak strength loss was not observed with the addition of tire chips. At no addition of tire chips (0%) and with the 10% addition of tire chips, it is observed that the post peak strength loss is minimal with reinforcement. From studies available in the literature, high values of friction angle (as high as 68°) were observed for the tire shred mixed with sand (Foose et al. 1996). Tatlisoz (1998) found that the interface shear parameters of reinforcement-sand and reinforcement- silty sand are as high as 50° with apparent cohesion equal to 30 kPa.

Table 4.3: Efficiency of geogrid with respect to cohesion and friction angle for tire chip mixed NFA

%Tire chips	Adhesion, Ca (kPa)	Interface friction angle, δ ($^\circ$)	Cohesion, C (kPa)	Internal friction angle, ϕ ($^\circ$)	E_c (%)	E_ϕ (%)
0	21.7	41.2	21.1	46.7	102	82.5
10	22.2	42.5	24.4	45.5	91	90
30	22.5	47.2	14.9	50.1	151	90
60	25.9	43.4	31.3	48	83	85

30% addition of tire chips has a greater adhesion with the geogrid, whereas mixtures with other percentages have adhesion ranging between 80-105% of cohesion. All the mixtures have an interface friction angle ranging 80-90% of friction angle.

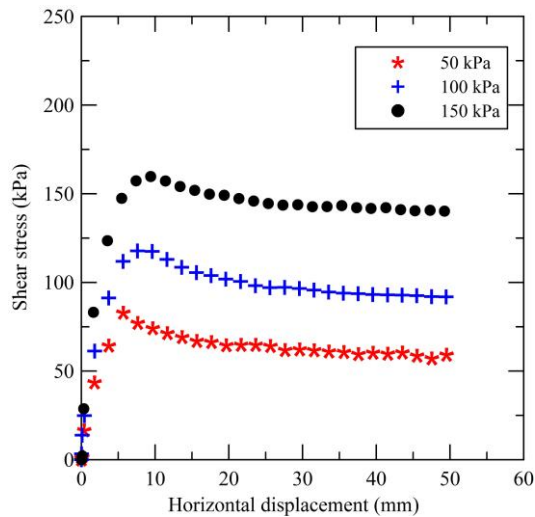
Interaction coefficient is calculated using Eq. 4.5 for the different percentage mixtures of tire chips with NFA. Table 4.4 gives the interaction coefficient of geogrid with the tire chip mixed NFA.

From Table 4.4, it is observed that high interface shear strengths are retained with the introduction of geogrid. For the 30% addition of tire chips to the NFA in the reinforced case, interfacial shear strength is equal to 98% of direct shear strength.

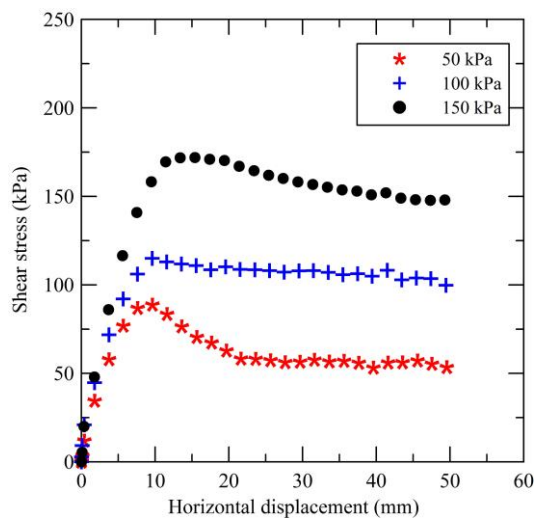
Table 4.4: Interaction coefficient of geogrid (R_i) at peak state

	0%	10%	30%	60%
Normal stress (kPa)	R_i	R_i	R_i	R_i
50	0.88	0.90	1.02	0.84
100	0.86	0.90	0.97	0.84
150	0.85	0.90	0.95	0.84
Average R_i	0.86	0.90	0.98	0.84

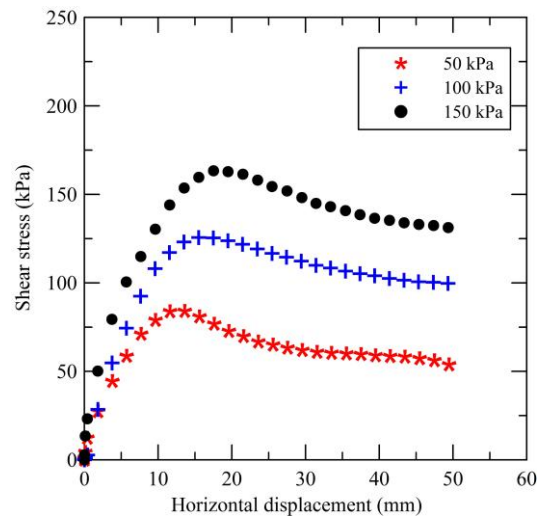
Figure 4.19 gives the variation of direct shear stress vs. the horizontal displacement of the box having RPA mixed with different percentages of tire chips. The combined shear strength envelopes for 10%, 30% and 60% tire chips mixed RPA samples are given in Fig 4.19(d).



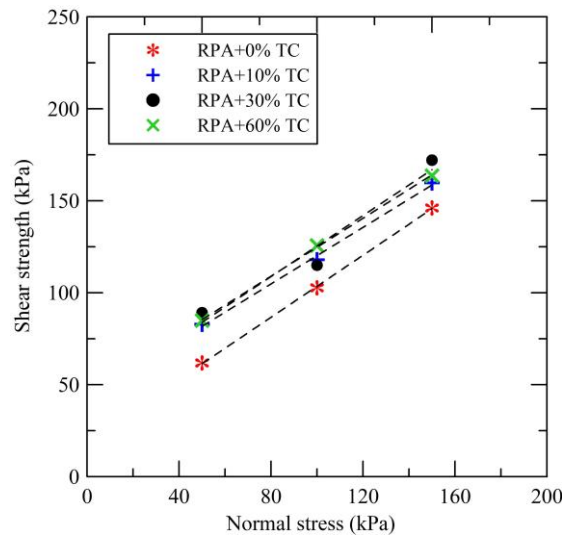
(a)



(b)



(c)

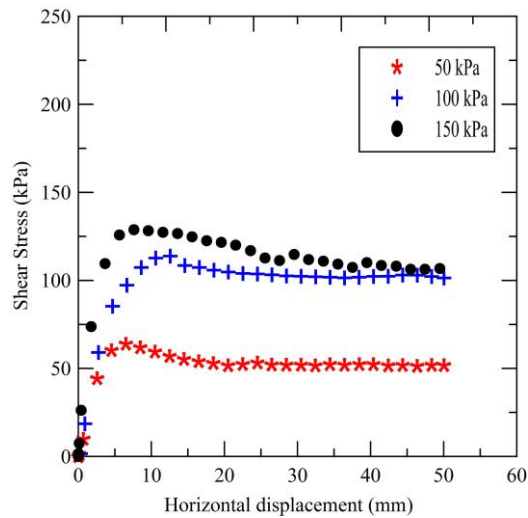


(d)

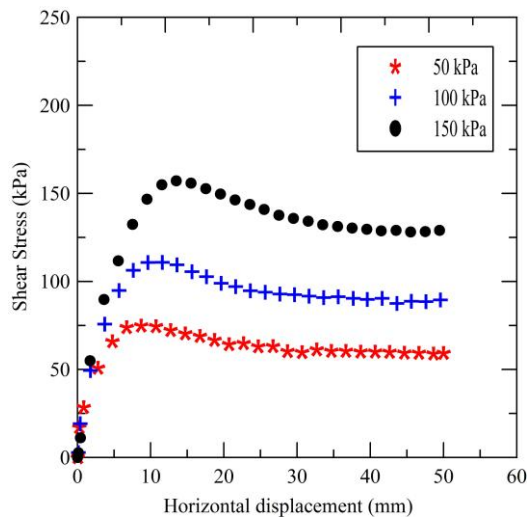
Fig 4.19(a) Shear stress vs. horizontal displacement of box for unreinforced RPA with 10% tire chips addition (b) Shear stress vs. horizontal displacement curve of box for unreinforced RPA with 30% tire chips addition (c) Shear stress vs. horizontal displacement curve of unreinforced RPA with 60% tire chips addition (d) Peak shear strength envelopes for the different amount tire chips and RPA

As for the case of NFA, the displacement to reach the failure is increased with the addition of tire chips to RPA. The displacements for the shear failure ranges from 5mm-10mm, 10mm-13mm, and 13mm-18mm for 10%, 30% and 60% addition of tire chips with NFA respectively at normal stresses of 50 kPa, 100 kPa and 150kPa. Fig 4.19(d) indicates that the addition of tire chips to RPA increases the shear strength. 30% and 60% additions lead to nearly equal shear strength.

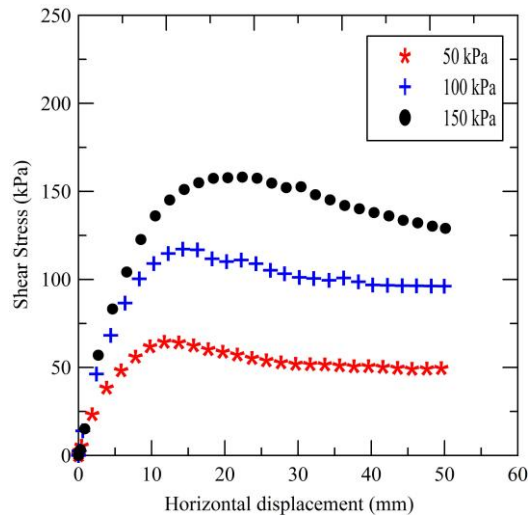
Figs 4.20 (a), (b) and (c) shows the interface shear stress vs horizontal displacement of the box with RPA mixed with different percentages of tire chips. The interface behavior RPA and tire chip mixtures with geogrid is found to be similar to that of mixtures of NFA and tire chips with geogrid. From Fig 4.20(d), higher interface shear strength of geogrid and mixtures are observed for 30% and 60% mixes. The horizontal displacement of box to reach the failure increased with the increase in tire chips content. The ranges of horizontal displacement to reach failure peak state for 10%, 30% and 60% are equal to 6-12 mm, 8-15 mm and 10-20 mm, respectively, for the range of normal stresses considered in the study.



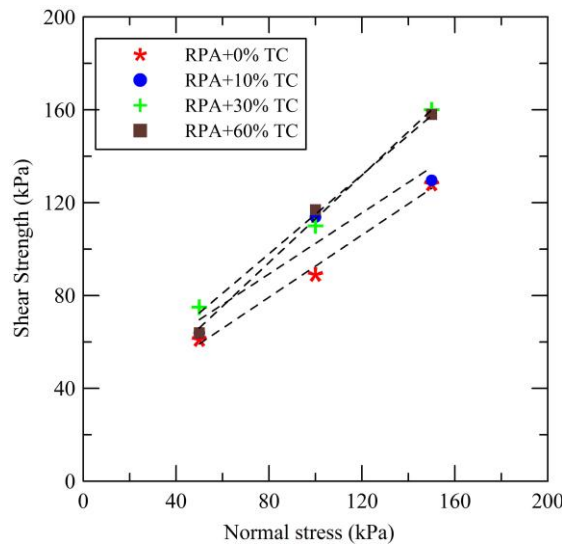
(a)



(b)



(c)



(d)

Fig 4.20(a) Shear stress vs. horizontal displacement of box for reinforced RPA with 10% tire chips addition (b) Shear stress vs. horizontal displacement curve of box for reinforced RPA with 30% tire chips addition (c) Shear stress vs. horizontal displacement curve of reinforced RPA with 60% tire chips addition (d) Peak interface shear strength envelopes for the different amount tire chips and RPA

Table 4.5 gives the direct shear and interface shear parameters obtained for RPA and tire chip mixtures along with the efficiency of geogrid with respect to cohesion and friction. Table 4.5 gives the direct shear and interface shear parameters for tire chip mixed RPA and efficiency of geogrid with respect to cohesion and friction. Efficiency of geogrid with respect to cohesion and friction are calculated using the Eq. 4.3 and Eq. 4.4.

Table 4.5: Efficiency of geogrid with respect to cohesion and friction for tire chip mixed RPA

% Tire chips	Adhesion, C_a (kPa)	Interface friction angle, δ ($^{\circ}$)	Cohesion, C (kPa)	Internal friction angle, ϕ ($^{\circ}$)	E_c (%)	E_{ϕ} (%)
0	15	36.8	19.2	40.1	78	88
10	25.6	33.8	43.3	37.5	60	87
30	30	40.3	42.2	39.7	72	102
60	19	43.2	46	38.2	41	119

Table 4.5 signifies that the adhesion between the tire chips mixed RPA and geogrid are comparably lower than that of the cohesion between the RPA particles. While the interface friction angle is close to that of the friction angle between RPA particles.

Interface coefficient of geogrid with tire chip mixed RPA is calculated using Eq. 4.5 and the results are presented in Table 4.6. Table 4.6 indicates that the interaction coefficient is higher for both 30% and 60%. Nearly 90% of the direct shear strength is being achieved with the introduction of geogrid.

Table 4.6: Interface interaction coefficient of geogrid with tire chip mixed RPA

	0%	10%	30%	60%
Normal stress (kPa)	Ri	Ri	Ri	Ri
50	0.85	0.72	0.86	0.77
100	0.87	0.77	0.91	0.90
150	0.87	0.79	0.94	0.97
Average Ri	0.86	0.76	0.90	0.88

Chapter 5

Conclusions

Interface shear tests were performed on geogrid and fly ash with two gradations (NFA and RPA). The results are compared with interface properties of geogrid and locally available sand. The following are the conclusions drawn from this study.

1. NFA is composed of coarse, angular particles with sizes varying in the range of silty sands to poorly-graded sand (SP). Morphological studies confirm that the particles of NFA are angular. It consists of 62% of SiO_2 , 21% of Al_2O_3 , 6% of Fe_2O_3 , and 4.9% of CaO . Specific gravity is equal to 2.54. Higher specific gravity than that of typical fly ashes is due to presence of higher content of Fe_2O_3 .
2. RPA is composed of spherical and angular particles, and classified as poorly-graded sand with little non-plastic fines (SP-SMN). It consists of 59% of SiO_2 , 19.5% of Al_2O_3 , 15.3% of Fe_2O_3 , and 3.1% of CaO . The chemical composition shows that the RPA is of Class-F type. Specific gravity is equal to 2.01.
3. Sand is poorly-graded type (SP) and composed of coarse and angular particles. Specific gravity is equal to 2.64.
4. The compaction studies conclude that the compaction curves of NFA, sand, and RPA are similar to that of granular soils. A dumb-bell shaped curve is obtained for all the samples.
5. The compaction studies on tire chips mixed with NFA and RPA showed a decrease in the unit weight with the addition of tire chips as expected. But, the shear strength parameters showed an increase with the addition of tire chips.
6. The direct shear results of NFA, sand and RPA are quite comparable. The shear strength (or) failure envelopes suggests that all the three namely NFA, sand, and RPA have comparable shear strengths. This justifies the use of NFA and RPA as a

backfill material at 90-95% relative compaction in place of conventional fill material.

7. The interfacial shear strengths of NFA, sand, and RPA are also quite high and comparable with that of sand at a relative compaction of 90-95%.
8. The efficiency of the geogrid with respect to cohesion (E_c) and friction angle (E_ϕ) for NFA, sand, and RPA are equal to 102% and 82.5%, 54% and 104%, and 130% and 79.7%, respectively.
9. The interaction coefficient (R_i) of the geo-grid for NFA, Sand and RPA are equal to 0.87, 0.92 and 0.90, respectively.
10. The interfacial shear strength of tire chips mixed NFA, and tire chips mixed RPA are tested with different mix proportions equal to 10%, 30% and 60% (by weight of dry fly ash).
11. The direct shear strength and interfacial shear strength of tire chips mixed NFA, and tire chips mixed RPA are experimented with different mix proportions like 10%, 30% and 60% (by weight of dry fly ash). 30% and 60% tire chips mixed with NFA and RPA give almost equal direct shear strengths. The mix with 30% tire chips is found to be the optimum mix which gives higher interfacial shear strength for both fly ashes considered in the study (NFA and RPA).
12. The efficiency of geogrid for tire chip NFA with respect to cohesion (E_c) and friction (E_ϕ) are found to be in the range of 80-150%, whereas for RPA it is in the range of 40-120%.
13. The interaction coefficients of geogrid (R_i) for 10%, 30% and 60% tire chips mixed with NFA are equal to 0.9, 0.98 and 0.84, respectively. While for tire chips mixed with RPA, the interaction coefficients are equal to 0.76, 0.90 and 0.88, respectively.

Based on the interface shear properties of geogrid and fly ash/fly ash-tire chip mixtures, it can be concluded that the composite material of fly ash and tire chips can be a competent material for backfill applications. However, other properties like compressibility, permeability, pH, pullout resistance, etc. should also be studied to confirm their suitability for this application.

References

- [1] Adamska, K.Z. (2006), “Shear strength parameters of compacted fly ash–HDPE geomembrane interfaces,” *Journal of Geotextiles and Geomembranes*, Vol. 24, pp. 91–102.
- [2] American Society for Testing and Materials, (ASTM) D2487-11, “Standard practice for classification of soils for engineering purposes (Unified Soil Classification System)”.
- [3] American Society for Testing and Materials, (ASTM) D5321-08, “Standard test method for determining the coefficient of soil and geosynthetic or geosynthetic and geosynthetic friction by direct shear method”.
- [4] American Society for Testing and Materials, (ASTM) D698-12, “Standard test methods for laboratory compaction characteristics of soil using standard effort”.
- [5] American Society for Testing and Materials, (ASTM) D854-10, “Standard test methods for specific gravity of soil solids by water Pycnometer”.
- [6] Anubhav and Basudhar, P.K. (2010), “Modeling of soil–woven geotextile interface behavior from direct shear test results,” *Journal of Geotextiles and Geomembranes*, Vol. 28, pp. 403–408.
- [7] Arora, S., Aydilek, A.H. (2005), “Class F fly-ash-amended soils as highway base materials,” *Journal of Materials in Civil Engineering*, ASCE, Vol. 17, No. 6, pp. 640-649.
- [8] Alam, J., and Akhtar, M.N. (2011), “Fly ash utilization in different sectors in Indian scenario,” *International Journal of Emerging trends in Engineering and Development*, Issue 1, Vol. 1, pp. 1-14.
- [9] Athanapoulos, A.G. (1996), “Results of direct shear tests on geotextile reinforced cohesive soil,” *Journal of Geotextiles and Geomembranes*, Vol. 14, pp. 619—644.
- [10] Attom, M. (2006), “The use of shredded waste tires to improve the geotechnical engineering properties of sand,” *Environ Geol*, Vol. 49, pp. 497–503.
- [11] Ayothiraman, R., and Meena, A.K. (2011), “Improvement of subgrade soil with shredded waste tires,” *Proceedings of Indian Geotechnical Conference December 15-17, Kochi (Paper No. H-033)*.

- [12] Bosscher, P.J., Edil, T.B., and Kuraoka, S. (1997), "Design of highway embankments using tire chips," *Journal of Geotech Geoenvironmental Engineering (ASCE)*, Vol. 123, No. 4, pp. 295–304.
- [13] Cabalar, A.F. (2011), "Direct shear tests on waste tire-sand mixtures," *Geotech Geol Engg. (Springer)*, Vol. 29, pp. 411-418.
- [14] Central electricity authority (CEA) report, (2014), "Fly ash generation at coal/lignite based thermal power stations and its utilization in the country", New Delhi.
- [15] Cetin, B., Aydilek, A.H., Li, L. (2014), "Trace metal leaching from embankment soils amended with high-carbon fly ash," *Journal of Geot and Geoenv Engg, ASCE*, Vol. 140, pp. 1-13.
- [16] Das, S.K. and Yudbir (2005), "Geotechnical characterization of some Indian fly ashes," *Journal of Materials in Civil Engineering ASCE*, Vol. 17, pp. 544-552.
- [17] Edinçliler, A., Ayhan, V. (2010), "Influence of tire fiber inclusions on shear strength of sand," *Geosynthetics International*, 2010, Vol. 17, No. 4, pp. 183-192.
- [18] Foose, G.J., Benson, C.H., Bosscher, P.J. (1996), "Sand reinforced with shredded waste tires," *Journal of Geotechnical Engineering*, Vol. 122, pp. 760-767.
- [19] Ghazavi, M. and Masoud, A. (2005), "Influence of optimized tire shreds on shear strength parameters on sand," *International Journal of Geomechanics, ASCE*, Vol. 5, pp. 58-65.
- [20] Hillman, R.P. and Stark, T.D. (2001), "Shear strength characteristics of PVC geomembrane-geosynthetic interfaces," *Geosynthetics International*, Vol. 8, No. 2, pp. 135-162.
- [21] Huang, H. W. (1990), "The use of bottom ash in highway embankments, subgrade, and subbases," *Joint Highway Research Project, Final Report, FHWA/IN/JHRP-90/4*, Purdue University, W. Lafayette, Indiana.
- [22] Japan Automobile Tyre Manufacturers Association (2007) *Tire Recycling Handbook*. Japan Automobile Tyre Manufacturers Association, Tokyo, Japan, p. 25.
- [23] Kim, B., Prezzi, M., Salgado, R. (2005), "Geotechnical properties of fly and bottom ash mixtures for use in highway embankments," *Journal of Geotechnical and Geoenvironmental Engineering, ASCE*, Vol. 131, No. 7, pp. 914-924.
- [24] Kim, H., Lee, M.S., Umashankar, B., Prezzi, M., Siddiki, N.Z. (2009), "Compaction quality control of fly and bottom ash mixture embankment using dynamic cone penetrometer and lightweight deflectometer", pp. 1-21.

- [25] Lee, J. H., Salgado, R., Bernal, A., Lowell, C.W. (1999), "Shredded tires and rubber-sand as lightweight backfill," *Journal of Geotech and Geoenviron Engineering*, Vol. 125, No.2, pp. 132-141.
- [26] Liu, C.N., Zornberg, J.G., Chen, T.C., Tsong-chia, Ho, Y.H., Lin, B.H. (2010), "Behavior of Geogrid-Sand Interface in Direct Shear Mode," *J. Geotech. Geoenviron. Engg.*, Vol. 135, No. 12, pp. 1863-1871.
- [27] Martin, J.P., Collins, R.A., Browning, J.S., Biehl, F.J. (1990), "Properties and use of fly ashes for embankments," *Journal of Energy Eng.*, Vol. 116, No. 2, pp. 71-86.
- [28] Marto, A., Latifi, N., Moradi, R., Oghabi, M., Zolfeghari, S.Y. (2013) "Shear properties of sand-tire chips mixtures," *Electronic Journal of Geotechnical Engineering*, pp. 325-334.
- [29] Naeini, S.A., Khalaj, M., Izadi, E. (2012), "Interfacial shear strength of silty sand-geogrid composite," *ICE, Geotechnical Engineering*, Vol. 166, Issue GE1, pp. 67-75.
- [30] Palmeira, E.M. (2009), "Soil-geosynthetic interaction: Modelling and analysis," *Geotextiles and Geomembranes*, Vol. 27, pp. 368-390.
- [31] Praveen, K. and Shalendra, P.S. (2008), "Fiber-reinforced fly ash subbases in rural roads," *Journal of Transportation Engg, ASCE*, Vol. 134, pp. 171-180.
- [32] Rai, A.K., Paul, B., Singh, G. (2010), "A study on backfill properties and use of fly ash for highway embankments," *Journal of Advanced Laboratory Research in Biology* Volume I, Issue II, pp. 110-114.
- [33] Roa, G.V. and Dutta, R.K. (2006), "Compressibility and strength behavior of sand-tire chip mixtures," *Geotech and Geol Eng. (Springer)*, Vol.24, pp. 711-724.
- [34] Rubber Manufacturers Association (2013) U.S. Scrap Tire Management Summary 2005-2009. Rubber Manufacturers Association, Washington DC, USA
- [35] Santos, F., Li, L., Li, Y., Amini, F. (2011), "Geotechnical properties of fly ash and soil mixtures for use in highway embankments," *World of Coal Association Conference (WOCA) Conference*.
- [36] Sarkar, R., Abbas, S.M., Shahu, J.T. (2011), "Geotechnical characterization of pond ash available in national capital region-Delhi," *International Journal of Earth Sciences and Engineering*, Vol. 04, No. 6, pp. 138-142.
- [37] Shulman, V.L. (2004) Tyre recycling. European Tyre Recycling Association (ETRA), Brussels, Belgium, *Rapra Review Reports*, Vol. 15, No. 7.
- [38] Singh, S.P. and Sharan, A. (2013), "Strength characteristics of compacted pond ash," *Geomechanics and Geoengineering: An International Journal*, DOI:10.1080/17486025.2013.772661.

- [39] Sheikh, N.M., Mashiri, M.S., Vinod, J.S., Tsang, H.H. (2013), "Shear and compressibility behavior of sand-tire crumb mixtures," *Journal of Materials in Civil Engineering*, ASCE, Vol. 25, No. 10, pp. 1366-1374.
- [40] Sridharan, A., Pandian, N.S., and Srinivas, S. and Subramanya Prasad, P. (2001a), Vol. 1: "Physical properties of Indian coal ashes," Technical report of task force on Characterization of fly ash submitted to Technology Mission-Fly Ash Disposal and Utilisation, Dept. of Science and Technology, Govt. of India.
- [41] Sridharan, A., Pandian, N.S., Subramanya Prasad, P. and Srinivas, S. and (2001b), Vol. 2: "Chemical properties of Indian coal ashes," Technical report of task force on Characterization of fly ash submitted to Technology Mission-Fly Ash Disposal and Utilization, Dept. of Science and Technology, Govt. of India.
- [42] Sridharan, A., Pandian, N.S., and Srinivas, S. (2001c), "Compaction behavior of Indian coal ashes," *Ground improvement*, Vol. 5, No. 1, pp. 13-22.
- [43] Sridharan, A., Pandian, N.S., and Chitti Babu, G. (2001d), Vol.4: "Strength Behavior of Indian Coal Ashes," Technical report of task force on Characterization of fly ash submitted to Technology Mission-Fly Ash Disposal and Utilization, Dept. of Science and Technology, Govt. of India.
- [44] Sridharan, A., Pandian, N.S., Subramanya Prasad, P. (2001e), Vol.6: "Consolidation and permeability behavior of Indian coal ashes," Technical report of task force on Characterization of fly ash submitted to Technology Mission-Fly Ash Disposal and Utilization, Dept. of Science and Technology, Govt. of India.
- [45] Sridharan, A., Pandian, N.S., and Srinivas, S. (2001f), Vol. 3: "Compaction behavior of Indian coal ashes," Technical report of task force on characterization of fly ash submitted to Technology Mission-Fly Ash Disposal and Utilization, Dept. of Science and Technology, Govt. of India.
- [46] Sridharan, A. and Prakash, K. (2007), Text book on "Geotechnical engineering characterization of coal ashes," CBS publishers, p. 10.
- [47] Tanchaisawat, T., Bergado, D.T., Voottipruex, P., Shehzad, K. (2009), "Interaction between geogrid reinforcement and tire chip-sand lightweight backfill," *Journal of Geotextiles and Geo-membranes*, Vol. 28, pp. 119-127.
- [48] Tatlisoz, N., Edil, T.B., Benson, C.H. (1998), "Interaction between reinforcing geosynthetics and soil-tire chip mixtures," *Journal of Geotech and Geoenvironmental Engineering*, Vol. 124, No. 11, pp. 1109-1119.
- [49] Tuna, S.C. and Altun, S. (2012) "Mechanical behaviour of sand-geotextile interface," *Scientia Iranica, Transactions A: Civil Engineering*, Vol. 19, No. 4, pp. 1044-1051.

- [50] Tweedie, J.J., Humphrey, D.N., Sandford, T.C. (1998), "Tire shreds as lightweight retaining wall backfill: Active conditions," *Journal of Geotech and Geoenvironmental Engineering*, Vol. 124, No. 11, pp. 1061-1070.
- [51] Umashankar, B., Yoon, S., Prezzi, M., Salgado, R. (2014), "Pullout response of uniaxial geogrid in tire shred-sand mixtures," *Geotech and Geol Eng. Springer*, Vol. 32, pp. 505-523.
- [52] Umashankar, B. and Prezzi, M. (2010), "Interaction of ribbed-metal-strip reinforcement with tire shred-sand mixtures," *Geotech Geol Eng*, Vol. 28, pp. 147-163.
- [53] Umashankar, B., Prezzi, M., Varenaya, K.D., Salgado, R. (2014), "Shear strength of tyre chip-sand and tyre shred-sand mixtures," *Geotech Eng*, In Print.